KONA Powder and Particle Journal No. 33 (2016) 179–202/Doi:10.14356/kona.2016024 Review Paper

Developments of Blocking Filtration Model in Membrane Filtration †

Eiji Iritani* and Nobuyuki Katagiri

[1] *Department of Chemical Engineering, Nagoya University, Japan*

Abstract

Blocking filtration laws consist of four different filtration mechanisms: complete blocking, standard blocking, intermediate blocking, and cake filtration. Blocking filtration laws for describing both the pore blocking and cake formation have been extensively employed over the past several decades to evaluate the increase in filtration resistance with the progress of filtration in the field of classical particulate filtration. In recent years, blocking filtration laws become widely used also in membrane filtration such as microfiltration and ultrafiltration of colloids. This paper gives an overview of the developments of blocking filtration laws and equations under constant pressure and constant rate conditions reported for the filtrate flow of Newtonian and non-Newtonian fluids. The fouling index evaluating the degree of membrane fouling was examined on the basis of the blocking filtration equations. The blocking filtration laws were reexamined to extend the range of their application. Moreover, various combined models developed based on the blocking filtration laws were introduced for describing more rigorously the complicated filtration behaviors controlled by more than one mechanism which occurs successively or simultaneously.

Keywords: membrane fouling, pore blocking, blocking filtration law, cake filtration, membrane filtration, filtration rate

1. Introduction

Membrane filtration processes such as microfiltration and ultrafiltration of dilute colloids play an increasingly important and indispensable role in widely diversified fields ranging from industry to drinking water production, treatment of domestic and industrial effluents, and production of water suitable for reuse. While membrane filtration is a key process which has the widespread application, it is generally recognized that one of the major drawbacks to more widespread use of membrane filtration is a significant increase in the filtration resistance known as membrane fouling, resulting in a dramatic flux decline over time under constant pressure conditions or a remarkable pressure rise over time under constant rate conditions. The membrane fouling is affected by several factors, e.g., pore blocking and/or pore constriction (Hermans and Bredée, 1935, 1936; Grace, 1956; Shirato et al., 1979; Hermia, 1982; Iritani et al, 1992, 2009, 2013), cake formation (Reihanian et al., 1983; Chudacek and Fane, 1984; Iritani et al., 1991a, 2014a, b; Nakakura et al., 1997; Mohammadi et al., 2005; Thekkedath et al., 2007; Sarkar, 2013; Salinas-Rodriguez et al., 2015), solute adsorption (Fane et al., 1983; Iritani et al., 1994), and concentration polarization (Kimura and Sourirajan, 1967; Vilker et al., 1981). Initially, foulants smaller than the pore size of membrane deposit or adsorb onto the pore walls, thereby leading to the pore constriction. This induces a significant reduction in the cross-sectional area available to the filtrate flow. In contrast, larger foulants deposit or adsorb onto the pore entrances, resulting in a marked increase in the filtrate flow resistance. In either case, the pore constriction and pore plugging are followed by the formation of filter cake accumulating on the membrane surface, thus severely increasing the filtration resistance. Therefore, it is essential to elucidate the underlying mechanism controlling the membrane fouling such as the pore constriction, pore plugging, and cake formation during the course of membrane filtration.

So far, a number of models have been proposed to describe the fouling of filter medium during the classical liquid filtration. The theory of cake filtration in which the filter cake forms on the surface of filter medium was initially established by Ruth (1935, 1946) and then extended to deal with the case of the compressible filter cake, as referred to as the modern filtration theory (Grace, 1953;

† Received 27 August 2015; Accepted 25 September 2015
J-STAGE online 28 February 2016
[1] Furo-cho, Chikusa-ku, Nagoya 464-8603, Japan
* Corresponding author: Eiji Iritani;
E-mail: iritani@nuce.nagoya-u.ac.jp
TEL: +81-52-789-3374 FAX: +81-52-789-4531

Tiller, 1953; Okamura and Shirato, 1955; Tiller and Shirato, 1964; Shirato et al., 1969).

The classical blocking filtration laws describe three types of physical mechanisms controlling the blockage of membrane pores, in addition to the cake filtration model. The blocking filtration laws were originally presented by Hermans and Bredée (1935, 1936) and later systematized by Grace (1956), Shirato et al. (1979), and Hermia (1982). The model consists of four different filtration mechanisms: complete blocking, standard blocking, intermediate blocking, and cake formation. Among them, both complete and intermediate blocking laws describe the pore plugging due to foulants reaching the top surfaces of pores. In contrast, the standard blocking law deals with the pore constriction caused by the deposition of foulants onto the pore wall. Interestingly enough, these four filtration mechanisms reduce to a common differential equation with different values of power index. While blocking filtration laws are summarized in quite simple mechanisms, still present today they provide a powerful tool to reasonably evaluate the increasing behavior of filtration resistance in liquid filtration of relatively dilute suspension. Nowadays, blocking filtration laws have become widely used in the analysis of the flux decline behaviors observed not only in classical liquid filtration but also in membrane filtration such as microfiltration and ultrafiltration. Therefore, it is considered that there is a significant value to have an overview of the developments of blocking filtration laws and the related mechanisms.

This review paper initially describes the classical blocking filtration laws derived under constant pressure conditions. Then, the blocking filtration laws are extended to be applied to constant rate (flux) filtration and are generalized through the inclusion of filtrate (permeate) flow of non-Newtonian fluids. A common characteristic filtration form derived from the blocking filtration laws is revisited by considering the membrane pore fouling represented by Kozeny-Carman equation describing the flow through the granular bed. The paper explains that the blocking filtration laws are made available for evaluating the degree of membrane fouling, e.g., the maximum filtrate volume and the fouling index such as SDI and MFI. Finally, the combined models stemming from the blocking filtration laws are described to reasonably evaluate two fouling mechanisms occurring sequentially or simultaneously, which are frequently observed in the actual processes of membrane filtration of colloids. Specifically, much emphasis is placed on the combination of membrane pore blockage and cake formation on the membrane surface. These combined model can approximate highly complicated membrane fouling behaviors often encountered in membrane filtration.

2. Blocking filtration law

2.1 Mechanism of blocking filtration

Blocking filtration laws are applied to four different fouling patterns for describing the deposit of particles on filter media and membranes, as schematically illustrated in **Fig. 1**. The complete, intermediate, and standard blocking laws describe the blocking of membrane pores, while the cake filtration law is applied to the description of the growth of filter cake comprised of particles accumulating on the membrane. For simplicity, it is postulated that the membrane consists of parallel pores with constant diameter and length. Both the complete and intermediate blocking laws are applicable in case that the particle diameter is larger than the pore size. Thus, each particle reaching the membrane due to convection is inevitably trapped on the membrane surface in either case. However, pore blocking behaviors are substantially different from each other. In the complete blocking law, it is assumed that each particle blocks an open pore completely, as shown in **Fig. 1(a)**. When more appropriate, it is assumed that the probability that a particle blocks an open pore is constant during the course of filtration, considering the possibility that a particle deposits on the membrane surface other than pores. Therefore, the number of blocked pores is directly proportional to the filtrate volume v per unit effective membrane area. The variation of the number of open pores during the course of filtration is given by $(N_0' - xv)$, where N_0' is the total number of open pores per unit effective membrane area at start of filtration, x is the number of particles blocking pores per unit filtrate volume. Since

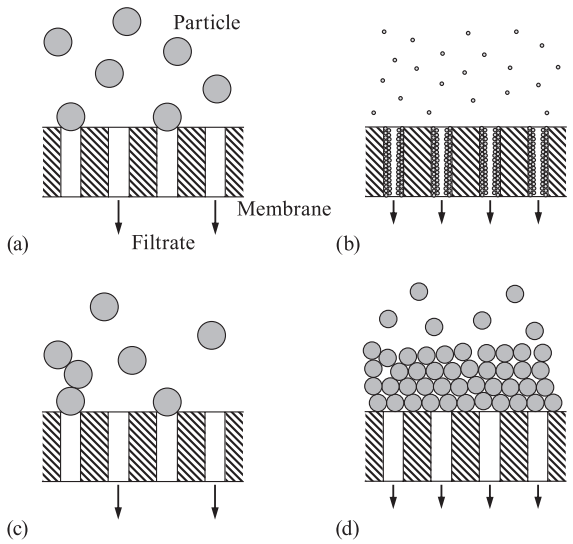

Fig. 1 Schematic view of four fouling patterns in blocking filtration laws: (a) complete blocking law, (b) standard blocking law, (c) intermediate blocking law, and (d) cake filtration law.

the filtration rate J is directly proportional to the number of open pores, it can be written as

$$J = \frac{dv}{dt} = k_c p(N_0' - xv) \tag{1}$$

where t is the filtration time, k_c is the proportional constant, and p is the applied filtration pressure. Differentiating Eq. (1) under the constant pressure condition ($p = p_0$ = const.), one obtains

$$\frac{d^2t}{dv^2} = k_c p_0 x\left(\frac{dt}{dv}\right)^2 = K_b\left(\frac{dt}{dv}\right)^2 \tag{2}$$

where K_b (= $k_c p_0 x$) is the blocking constant for complete blocking law.

However, in practice, the probability that a particle blocks an open pore varies with v during the course of filtration. As the number of open pores decreases due to the progress of filtration, particles newly reaching the membrane may deposit onto the particles that have already blocked the open pores, as shown in **Fig. 1(c)**. In the intermediate blocking law, it is assumed that the rate of pore blocking is proportional to the number of open pores, and thus dN'/dv may be written as

$$\frac{dN'}{dv} = -K_i N' \tag{3}$$

where N' is the number of open pores per unit effective membrane area at the filtrate volume v per unit effective membrane area, and K_i is the blocking constant for intermediate blocking law. Integrating Eq. (3), the number of open pores becomes $N_0' \exp(-K_i v)$. Consequently, the filtration rate is given by

$$J = \frac{dv}{dt} = k_c p N_0' \exp(-K_i v) \tag{4}$$

Differentiating Eq. (4) under the constant pressure condition, one obtains (Hermia, 1982)

$$\frac{d^2t}{dv^2} = K_i\left(\frac{dt}{dv}\right) \tag{5}$$

Although the intermediate blocking law had been considered to be empirical over the years (Grace, 1956), Hermia (1982) originally verified the theoretical background of the intermediate blocking law by considering the decrease in the probability blocking membrane pores with the progress of filtration. Around the same time, Hsu and Fan (1984) proposed the intermediate blocking equations applicable to constant rate filtration on the basis of the stochastic model (pure birth model) in order to use them in the analysis of sand filtration behaviors. Iritani et al. (1991b) derived the intermediate blocking equations for constant pressure filtration based on the stochastic model by considering the probabilistic event with the progress of the filtrate volume v per unit membrane area instead of the filtration time t because the number of particles reaching the membrane is proportional to v in the case of constant pressure filtration. Fan et al. (1985a, b) modified the intermediate blocking equations based on the birth-death model. In the model, scouring of particles blocking pores was also taken into consideration as the death process.

In the standard blocking law shown in **Fig. 1(b)**, the particle diameter is considerably smaller than the pore size. Therefore, solid-liquid separation proceeds by the deposition of particles on the pore wall and the pore gradually constricts with the progress of filtration. For simplicity, it is postulated that the pore volume decreases proportionally to the filtrate volume v per unit membrane area. Consequently, the filtration rate under the constant pressure condition gradually decreases with decreasing pore size. On the assumption that the pore radius decreases by dr by obtaining an infinitesimal amount of filtrate volume dv per unit membrane area, the mass balance produces (Grace, 1956)

$$-2\pi L N_0' r\,dr = \frac{c}{1-\varepsilon_p}dv \tag{6}$$

where L is the membrane thickness, c is the volume of particles trapped per unit filtrate volume v per unit membrane area, and ε_p is the packing porosity of the particle layer formed on the pore wall. Integrating Eq. (6) from $r = r_0$ at $v = 0$ to $r = r$ at $v = v$, one obtains

$$\frac{r}{r_0} = \left(1 - \frac{K_s v}{2}\right)^{0.5} \tag{7}$$

where K_s is the blocking constant for standard blocking law and defined by

$$K_s = \frac{2c}{N' L \pi (1-\varepsilon_p) r_0^2} \tag{8}$$

In general, the relation between the average flow rate u and pore radius r can be given by the Hagen-Poiseuille law applicable to the laminar flow in a capillary, and it is written as

$$u = \frac{r^2 p}{8\mu L} \tag{9}$$

where μ is the viscosity of the filtrate. Thus, the filtration rate through the membrane comprised of capillaries can be described by

$$J_0 = N'\pi r_0^2 \frac{r_0^2 p_0}{8\mu L} \tag{10}$$

at the start of filtration;

$$J = N'\pi r^2 \frac{r^2 p}{8\mu L} \tag{11}$$

at any time of filtration, where the subscript "0" indicates

the initial value. Substituting Eqs. (10) and (11) into Eq. (7) under the constant pressure condition ($p = p_0$ = const.), one obtains

$$J = J_0\left(1-\frac{K_s}{2}v\right)^2 \tag{12}$$

Differentiation of Eq. (12) yields

$$\frac{d^2t}{dv^2} = K_s {J_0}^{0.5}\left(\frac{dt}{dv}\right)^{1.5} \tag{13}$$

The filtration data of most dilute suspensions is described by the standard blocking law.

In contrast to the pore blocking, in cake filtration shown in **Fig. 1(d)**, the filter cake consisted of the particles deposited on the membrane surface gradually grows as filtration proceeds. The filter cake is viewed as a kind of granular bed which produces the increase in the thickness with the progress of filtration, thereby resulting in the increase in the additional resistance to flow. According to the Ruth theory, the filtration rate J is given by (Ruth, 1935, 1946)

$$\frac{1}{J} = \frac{dt}{dv} = \frac{\mu\alpha_{av}\rho s}{p(1-ms)}(v+v_m) \tag{14}$$

where α_{av} is the average specific cake resistance, ρ is the density of filtrate, s is the mass fraction of solids in colloids, m is the ratio of the mass of wet to the mass of dry cake, and v_m is the fictitious filtrate volume per unit membrane area required to obtain the cake with the flow resistance equivalent to that of the membrane. Since both α_{av} and m are considered to be constant throughout the period of filtration under the constant pressure condition, Eq. (14) becomes

$$\frac{1}{J} = \frac{dt}{dv} = \frac{2}{K_v}(v+v_m) \tag{15}$$

where K_v (= $2p(1 - ms)/(\mu\alpha_{av}\rho s)$) is the Ruth coefficient in constant pressure cake filtration and constant (Ruth, 1935, 1946). Although the filter cake generally exhibits compressible behavior in which α_{av} varies with the applied filtration pressure, it should be noted that Eq. (15) is applicable to not only the incompressible cake but also compressible cake (Tiller and Cooper, 1960; Tiller and Shirato, 1964). Differentiating Eq. (15) with respect to the time t, one gets

$$\frac{d^2t}{dv^2} = \frac{2}{K_v} = K_c \tag{16}$$

where K_c (= $2/K_v$) is the blocking constant for cake filtration law.

Interestingly enough, Eqs. (2), (5), (13), and (16) derived for four different filtration mechanisms reduce to the following common differential equation (Hermans and Bredée, 1935, 1936; Grace, 1956).

$$\frac{d^2t}{dv^2} = k\left(\frac{dt}{dv}\right)^n \tag{17}$$

where k and n are constants. The value of the blocking index n depends on the mode of filtration mechanisms, and indicates 2.0 for complete blocking, 1.5 for standard blocking, 1.0 for intermediate blocking, and 0 for cake filtration. The constant k is the resistance coefficient depending on the properties of suspension, membrane, and the operating conditions in filtration such as the applied filtration pressure. It is found from Eq. (17) that the changing rate in the filtration resistance is proportional to the filtration resistance raised to a power n. When the blocking filtration laws are represented by using the filtration rate J (= dv/dt), Eq. (17) reduces to (Sun et al., 2003)

$$\frac{dJ}{dt} = -kJ^{3-n} \tag{18}$$

A double logarithmic plot of d^2t/dv^2 vs. dt/dv is depicted based on the flux decline behaviors in order to understand the membrane fouling mechanism of constant pressure filtration with the aid of Eq. (17). The fouling mode can be easily determined from the slope of a linear regression fitting to the plot. However, since d^2t/dv^2 is the second order differential of the filtration time t with respect to the filtrate volume v per unit membrane area, the value of n determined from the direct use of Eq. (17) is likely to be influenced by the noise in the experimental data measured as the cumulative filtrate volume v per unit membrane area vs. the time t. Nevertheless, this plot provides important information on the fouling mechanism of membranes, as mentioned later (Bowen et al., 1995; Iritani et al., 1995, 2014c).

Table 1 systematically edits mathematical equations derived for each blocking filtration law under the constant pressure condition and represents v as functions of t and the filtration rate J as functions of t or v (Hermans and Bredée, 1935, 1936; Grace, 1956). These expressions can be used as a means for identifying the membrane fouling mechanism, just like the double logarithmic plot of d^2t/dv^2 vs. dt/dv. The fouling pattern of membranes can be judged from the plots shown in **Fig. 2** based on the linear expressions. For example, if the membrane fouling is controlled by the complete blocking filtration mechanism, the plot of J vs. v and the semi-logarithmic plot of J vs. t should show straight lines. Thus, the predominant blocking filtration law describing membrane fouling pattern can be determined from the graphical expression best fitted based on a linear regression analysis.

Integration of Eq. (18) with respect to the filtration time t produces the relation between the filtration rate J vs. the time t (Herrero et al., 1997; Ho and Zydney, 1999). It should be noted that the standard blocking (n = 1.5), intermediate blocking (n = 1.0), and cake filtration (n = 0)

Table 1 Blocking filtration equations for constant pressure filtration

Function	(a) Complete blocking	(b) Standard blocking	(c) Intermediate blocking	(d) Cake filtration
$\frac{d^2t}{dv^2}=k\left(\frac{dt}{dv}\right)^n$	$n=2.0$	$n=1.5$	$n=1.0$	$n=0$
$v=f(t)$	$v=\frac{J_0}{K_b}\{1-\exp(-K_bt)\}$ (19)	$\frac{t}{v}=\frac{K_s}{2}t+\frac{1}{J_0}$ (22)	$K_iv=\ln(1+K_iJ_0t)$ (25)	$\frac{t}{v}=\frac{K_c}{2}v+\frac{1}{J_0}$ (28)
$J=f(t)$	$J=J_0\exp(-K_bt)$ (20)	$J=\frac{J_0}{\left(\frac{K_sJ_0}{2}t+1\right)^2}$ (23)	$K_it=\frac{1}{J}-\frac{1}{J_0}$ (26)	$J=\frac{J_0}{(1+2K_cJ_0^2t)^{1/2}}$ (29)
$J=f(v)$	$K_bv=J_0-J$ (21)	$J=J_0\left(1-\frac{K_s}{2}v\right)^2$ (24)	$J=J_0\exp(-K_iv)$ (27)	$K_cv=\frac{1}{J}-\frac{1}{J_0}$ (30)

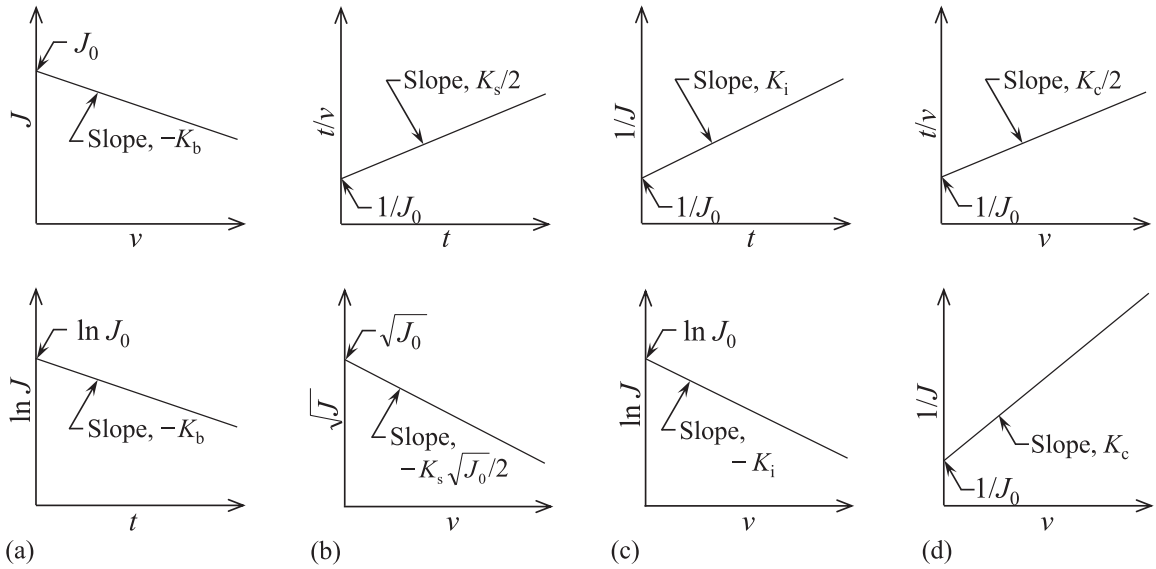

Fig. 2 Graphical identification of blocking filtration laws for constant pressure filtration: (a) complete blocking law, (b) standard blocking law, (c) intermediate blocking law, and (d) cake filtration law.

modes are represented as a common equation given by

$$J=\frac{J_0}{(1+k_jt)^{n_j}} \tag{31}$$

where k_j (= $k(2-n)J_0^{(2-n)}$) and n_j (= $1/(2-n)$) are constants. In contrast, in the case of the complete blocking law (n = 2), integrating Eq. (18), one obtains

$$J=J_0\exp(-kt) \tag{32}$$

Conventionally, the experimental data of the flux decline during the blocking filtration period have been analyzed by only one of above mentioned blocking filtration laws (Granger et al., 1985; Hodgson et al., 1993; Blanpain et al., 1993; Ruohomäki and Nyström, 2000; Gironès et al., 2006; Lee et al., 2008; de Lara and Benavente, 2009; Nandi et al., 2010; Li et al., 2012; Lim and Mohammad, 2012; Pan et al., 2012; Masoudnia et al., 2013, Palencia et al., 2014). Tettamanti (1982) proposed five blocking filtration laws by adding the adhesive filtration law in which the value of k in Eq. (17) is represented as zero. When a stepwise procedure is employed, the blocking filtration equation is derived in the form (Heertjes, 1957)

$$J=J_0\left(\frac{N'}{N'-axv}\right)^{-S_c} \tag{33}$$

where a and S_c are constants. In the case of complete blocking, a = 1.0 and S_c = 1.0. For partial blocking, a < 1.0 and S_c > 1.0. As the slurry concentration increases, a decreases and S_c increases, and both a and S_c depend on the form of pore and of the particle. In recent years, several problems are pointed out in applying the blocking filtra-

tion laws to the analysis of the experimental data of the flux decline during blocking filtration (Tien and Ramarao, 2011; Tien et al., 2014).

2.2 Blocking filtration equations for constant rate filtration

Although the membrane blocking research has been focused mostly on constant pressure filtration, which is easily tested on the laboratory scale, the membrane blocking in constant rate filtration is also crucially important from the viewpoint of the industrial level. While the flux decline behaviors are examined in constant pressure filtration, the pressure rising behaviors resulting from the increase in the filtration resistance are investigated in constant rate filtration in which the filtration rate is kept constant (Blankert et al., 2006; Liu and Kim, 2008; Sun et al., 2008; Mahdi and Holdich, 2013; Raspati et al., 2013).

The blocking filtration equations for constant rate filtration can be obtained in accordance with a procedure similar to that used in constant pressure filtration. For example, in complete blocking law, Eq. (1) is rewritten as

$$p = \frac{J}{k_c (N_0' - xv)} \tag{34}$$

Differentiating Eq. (34) with respect to v under constant rate condition ($J = J_0 = \text{const.}$), one gets

$$\frac{dp}{dv} = \frac{k_c x}{J_0} p^2 = \frac{K_b}{J_0 p_0} p^2 = K_{br} p^2 \tag{35}$$

where K_{br} ($= k_c x/J_0$) is the blocking constant for complete blocking law in constant rate filtration. Eventually, also in the case of constant rate filtration, four blocking filtration laws are represented by a common differential equation in the form (Grace, 1956)

$$\frac{dp}{dv} = k' p^{n'} \tag{36}$$

where k' and n' are constants. A power index n' is the blocking index which defines the filtration mechanism, and indicates the same value as constant pressure filtration for each blocking filtration law. **Table 2** lists the equations derived for constant rate filtration (Grace, 1956). Graphical indications are illustrated in **Fig. 3** and are employed in order to judge the blocking filtration law. The filtrate volume v per unit membrane area is directly proportional to the filtration time t in constant rate filtration, i.e., $v = J_0 t$. Consequently, it is also possible to identify the dominant blocking filtration law by plotting the data against t in place of v shown in **Fig. 3**.

The value of n' is 0 for cake filtration in which an incompressible filter cake forms during filtration. However, when the filter cake exhibits a compressible behavior, the use of Eq. (36) requires a considerable attention. Equation (14) is rewritten as

Table 2 Blocking filtration equations for constant rate filtration

Function	(a) Complete blocking	(b) Standard blocking	(c) Intermediate blocking	(d) Cake filtration
$\frac{dp}{dv} = k' p^{n'}$	$n' = 2.0$	$n' = 1.5$	$n' = 1.0$	$n' = 0$
$p = f(v)$	$\frac{p_0}{p} = 1 - \frac{K_b}{J_0} v$ (37)	$\left(\frac{p_0}{p}\right)^{1/2} = 1 - \frac{K_s}{2} v$ (38)	$\ln\left(\frac{p}{p_0}\right) = K_i v$ (39)	$\frac{p}{p_0} = 1 + K_c J_0 v$ (40)

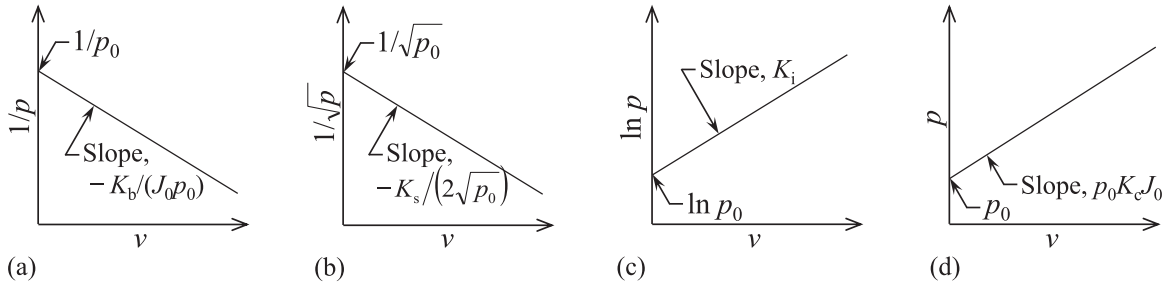

Fig. 3 Graphical identification of blocking filtration laws for constant rate filtration: (a) complete blocking law, (b) standard blocking law, (c) intermediate blocking law, and (d) cake filtration law.

$$p = \frac{\mu \alpha_{av} \rho s J}{1 - ms}(v + v_m) \tag{41}$$

The average specific cake resistance α_{av} in Eq. (41) is related to the applied filtration pressure p by (Sperry, 1921; Murase et al., 1987; Iritani et al., 2002; Zhou et al., 2015)

$$\alpha_{av} = \alpha_1 p^{n_1} \tag{42}$$

where α_1 and n_1 are constants, and n_1 is especially termed the compressibility coefficient of the filter cake. The higher the n_1-value, the more compressibility the cake is. Substituting Eq. (42) into Eq. (41), one obtains (Tiller, 1955; Shirato et al., 1968)

$$p^{1-n_1} = \frac{\mu \alpha_1 \rho s J}{1 - ms}(v + v_m) \tag{43}$$

Differentiation of Eq. (43) with respect to v under the constant rate conditions leads to

$$\frac{dp}{dv} = \frac{(1 - n_1)\mu \alpha_1 \rho s J}{1 - ms} p^{n_1} = k_1 p^{n_1} \tag{44}$$

where k_1 (= $(1 - n_1)\mu\alpha_1\rho sJ/(1 - ms)$) is a constant. Therefore, the value of n' in Eq. (36) is not 0 for constant rate cake filtration in which a compressible filter cake forms during filtration and increases as the compressible behaviors become more pronounced. If the compressibility coefficient n_1 is 1.0, as seen in highly compressible filter cake, the power index n' in the differential equation for cake filtration shows the same value as that derived for the intermediate blocking law, thereby leading to serious confusion.

Since v is directly proportional to the time t in constant rate filtration, Eq. (36) is rewritten as

$$\frac{dp}{dt} = k_2 p^{n'} \tag{45}$$

where k_2 is a constant. It should be noted that the characteristic differential equation can be represented also in the form (Hlavacek and Bouchet, 1993)

$$\frac{d^2 t}{dp^2} = k_1' \left(\frac{dt}{dp}\right)^{n_1'} \tag{46}$$

where k_1' and n_1' are constants. Equation (46) is similar to Eq. (17) in the form, by considering that p in Eq. (46) corresponds to v in Eq. (17). Alternatively, the characteristic form is represented by (Chellam and Xu, 2006; Chellam and Cogan, 2011)

$$\frac{d^2 p}{dv^2} = k_2' \left(\frac{dp}{dv}\right)^{n_2'} \tag{47}$$

where k_2' and n_2' are constants. Also in this case, the use of Eq. (47) requires a considerable attention in applying it to filtration forming compressible filter cakes. Chellam and Xu (2006) employed the expression of the average specific cake resistance α_{av} increasing with pressure p in the analysis of constant rate filtration behaviors, as described by

$$\alpha_{av} = \alpha_0 + \alpha_2 p \tag{48}$$

where α_0 and α_2 are constants, and α_0 is the average specific cake resistance at null stress. Eq. (48) has been applied to microbial suspensions, which exhibit highly compressible behaviors under relatively high pressure conditions. In this case, the value of exponent n_2' in Eq. (47) becomes 1.5, and thus is the same as the complete blocking law.

Blocking filtration equations applicable to variable pressure and variable rate filtration were proposed by Suarez and Veza (2000). For instance, in the complete blocking law, the relation among the filtration rate J, applied filtration pressure p, and filtrate volume v per unit membrane area can be obtained on the basis of Eq. (1) and thus is represented by

$$\frac{J}{p} = \frac{J_0}{p_0} - \frac{K_b}{p_0} v \tag{49}$$

The model adequately described the blocking filtration behaviors of effluent water from a municipal wastewater treatment plant.

2.3 Blocking filtration equations for filtrate of non-Newtonian fluids

When the filtrate flow presents with non-Newtonian behaviors, the analysis for blocking filtration law becomes even more complex than the filtrate flow of Newtonian fluids. In power-law non-Newtonian fluids, which are the simplest case, the rheological equation representing the relation between the shear stress τ and shear rate $\dot{\gamma}$ is written as

$$\tau = K \dot{\gamma}^N \tag{50}$$

where K is the fluid consistency index, and N is the fluid behavior index representing the intensity of non-Newtonian behaviors. When the fluid is characterized by Newtonian fluid, the value of N is equal to 1.0 and departs from 1.0 as non-Newtonian behaviors are more pronounced. The values of N less than 1.0 characterize pseudo-plastic or shear thinning fluids and melts. On the basis of Eq. (50), the relation between the average flow rate u and the tube radius r for power-law non-Newtonian fluids is given by (Kozicki et al., 1966)

$$u = \frac{N}{3N + 1}\left(\frac{p}{2KL}\right)^{1/N} r^{(N+1)/N} \tag{51}$$

When one puts N as 1.0 and K as the Newtonian viscosity μ, Eq. (51) reduces to the Hagen-Poiseuille equation applicable to Newtonian flow represented as Eq. (9).

While the number of open pores varies with the prog-

ress of filtration in both complete blocking and intermediate blocking laws, the radius of open pores remains constant since the start of filtration. Therefore, the forms of the blocking filtration equations for complete blocking and intermediate blocking laws are independent of the flow behaviors in pores, irrespective of the difference between Newtonian and non-Newtonian fluids. However, since the pore radius gradually decreases with the progress of filtration in the standard blocking law, the difference between Newtonian and non-Newtonian fluid is quite obvious, as inferred by Eq. (51). The filtration rates at the start and any time of filtration are, respectively, represented as

$$J_0 = N'\pi \frac{N}{3N+1}\left(\frac{p_0}{2KL}\right)^{1/N} r_0^{(3N+1)/N} \tag{52}$$

$$J = N'\pi \frac{N}{3N+1}\left(\frac{p}{2KL}\right)^{1/N} r^{(3N+1)/N} \tag{53}$$

Substituting Eqs. (52) and (53) into Eq. (7) under the constant pressure condition ($p = p_0 = \text{const.}$), one gets

$$J = J_0\left(1-\frac{K_s}{2}v\right)^{(3N+1)/2N} \tag{54}$$

Differentiating Eq. (54), one obtains (Shirato et al., 1979)

$$\frac{\mathrm{d}^2t}{\mathrm{d}v^2} = \frac{3N+1}{4N}K_s{J_0}^{2N/(3N+1)}\left(\frac{\mathrm{d}t}{\mathrm{d}v}\right)^{(5N+1)/(3N+1)} \tag{55}$$

The filtration rate in cake filtration is described by (Kozicki et al., 1968, 1972; Shirato et al., 1977, 1980; Murase et al., 1989)

$$\left(\frac{1}{J}\right)^N = \left(\frac{\mathrm{d}t}{\mathrm{d}v}\right)^N = \frac{K\gamma_{av}\rho s}{p(1-ms)}(v+v_m) \tag{56}$$

where γ_{av} is the average specific cake resistance for power-law non-Newtonian flow. Differentiating Eq. (56) with respect to v under the constant pressure condition ($p = p_0 = \text{cont.}$) where γ_{av} and m are treated as constant throughout the course of filtration, one obtains

$$\frac{\mathrm{d}^2t}{\mathrm{d}v^2} = \frac{K\gamma_{av}\rho s}{Np_0(1-ms)}\left(\frac{\mathrm{d}t}{\mathrm{d}v}\right)^{1-N} \tag{57}$$

Consequently, four blocking filtration laws for power-law non-Newtonian filtration under the constant pressure condition can be represented by a common differential equation with two constants k_N and n_N, as described by (Shirato et al., 1980; Hermia, 1982; Rushton, 1986)

$$\frac{\mathrm{d}^2t}{\mathrm{d}v^2} = k_N\left(\frac{\mathrm{d}t}{\mathrm{d}v}\right)^{n_N} \tag{58}$$

In the case of constant rate filtration, the characteristic form is represented as

$$\frac{\mathrm{d}p}{\mathrm{d}v} = k'_N p^{n'_N} \tag{59}$$

where k'_N and n'_N are constants. The blocking filtration equations are listed in **Table 3** for constant pressure and constant rate filtration processes for power-law non-Newtonian flow. In the case of constant pressure filtration, the complete and intermediate blocking filtration equations for the filtrate flow of non-Newtonian fluids are the same as those for the flow of Newtonian fluids and thus

Table 3 Blocking filtration equations for power-law non-Newtonian fluids-solids mixtures: (a) constant pressure filtration and (b) constant rate filtration

(a)

Function	Standard blocking	Cake filtration
$\frac{\mathrm{d}^2t}{\mathrm{d}v^2} = k_N\left(\frac{\mathrm{d}t}{\mathrm{d}v}\right)^{n_N}$	$n_N = \frac{5N+1}{3N+1}$	$n_N = 1-N$
$v = f(t)$	$v = \frac{2}{K_s}\left\{1-\left(\frac{N+1}{4N}K_sJ_0t+1\right)^{-2N/(N+1)}\right\}$ (60)	$\left\{K_cv+\left(\frac{1}{J_0}\right)^N\right\}^{(N+1)/N} - \left(\frac{1}{J_0}\right)^{N+1} = \frac{N+1}{N}K_ct$ (63)
$J = f(t)$	$J = J_0\left(\frac{N+1}{4N}K_sJ_0t+1\right)^{-(3N+1)/(N+1)}$ (61)	$\left(\frac{1}{J}\right)^{N+1} - \left(\frac{1}{J_0}\right)^{N+1} = \frac{N+1}{N}K_ct$ (64)
$J = f(v)$	$J = J_0\left(1-\frac{K_s}{2}v\right)^{(3N+1)/2N}$ (62)	$K_cv = \left(\frac{1}{J}\right)^N - \left(\frac{1}{J_0}\right)^N$ (65)

(b)

Function	Complete blocking	Standard blocking	Intermediate blocking	Cake filtration
$\frac{\mathrm{d}p}{\mathrm{d}v} = k_N{}'p^{n_N'}$	$n_N{}' = \frac{N+1}{N}$	$n_N{}' = \frac{3N+3}{3N+1}$	$n_N{}' = 1$	$n_N{}' = 0$
$p = f(v)$	$\left(\frac{p_0}{p}\right)^{1/N} = 1-\frac{K_b}{J_0}v$ (66)	$\left(\frac{p_0}{p}\right)^{2/(3N+1)} = 1-\frac{K_s}{2}v$ (67)	$\ln\left(\frac{p}{p_0}\right) = NK_iv$ (68)	$\frac{p}{p_0} = K_cJ_0^Nv+1$ (69)

they are omitted from the table. It should be stressed that the equations for Newtonian fluids is the special case of those for power-law non-Newtonian fluids.

Fig. 4 shows the experimental results of clarification filtration of dilute suspensions prepared by suspending diatomaceous earth in aqueous sodium polyacrylate exhibiting the behavior of power-law non-Newtonian fluid (Iritani et al., 1991b). The plots of $J^{2N/(3N+1)}$ vs. v yield linear relationships in accordance with Eq. (54) for the standard blocking law since the diameter d_p of the suspended solids is much smaller than the pore size d_m. As the solids mass fraction s in suspension decreases, the slope of straight line decreases and thus the filtrate volume obtained during clarification filtration increases.

2.4 Significance of blocking index *n* in blocking filtration laws

The unified characteristic form of blocking filtration laws is derived from four different filtration mechanisms. The blocking index n in Eq. (17) results in values of 2.0, 1.5, 1.0, and 0 for complete blocking, standard blocking, intermediate blocking, and cake filtration laws, respectively. However, in practice, the experimental data frequently exhibit the value other than these. Moreover, even though the pore size is much larger than the particle size, the blocking index n occasionally exhibits the value of 2.0. Therefore, from this point of view it is of significance to throw a new look at the underlying model of the characteristic form of blocking filtration laws.

In the blocking filtration model, for simplicity, it is assumed that the membrane consists of parallel cylindrical pores with constant diameter and length. However, in practice, the porous structure of most membranes is of a complex geometry with irregular pore morphology. The Kozeny-Carman equation can describe the flow through such a porous medium and is written as

$$J = \frac{\mathrm{d}v}{\mathrm{d}t} = \frac{\varepsilon^3}{k_0 S^2 (1-\varepsilon)^2} \cdot \frac{p}{\mu L} \tag{70}$$

where ε is the porosity, S is the specific surface area, and k_0 is the Kozeny constant. Iritani et al. (2007a) derived the characteristic form of blocking filtration laws on the basis of the Kozeny-Carman equation (70), by considering the variations of the porosity and the specific surface area of the membrane caused by the particle deposition within the porous membrane during filtration, as schematically illustrated in **Fig. 5**. The porosity ε in Eq. (70) decreases by particle deposition on the pore walls with the progress of filtration and is represented by

$$\varepsilon = \varepsilon_0 - K_p v = \left(1 - \frac{K_p v}{\varepsilon_0}\right)\varepsilon_0 \tag{71}$$

where ε_0 is the initial porosity of clean membrane, and K_p is a constant. The specific surface area S of the membrane in Eq. (70) also varies with the progress of filtration and it is assumed that S is described as

$$S^2(1-\varepsilon)^2 = \left(1 - \frac{K_p v}{\varepsilon_0}\right)^{\beta} S_0^2 (1-\varepsilon_0)^2 \tag{72}$$

where S_0 is the initial specific surface area of the clean membrane, and β is a constant which depends on the mode of the morphology of the deposit assemblages and defined as

$$\frac{D_s}{D_{s0}} = \left(\frac{D}{D_0}\right)^{\beta} \tag{73}$$

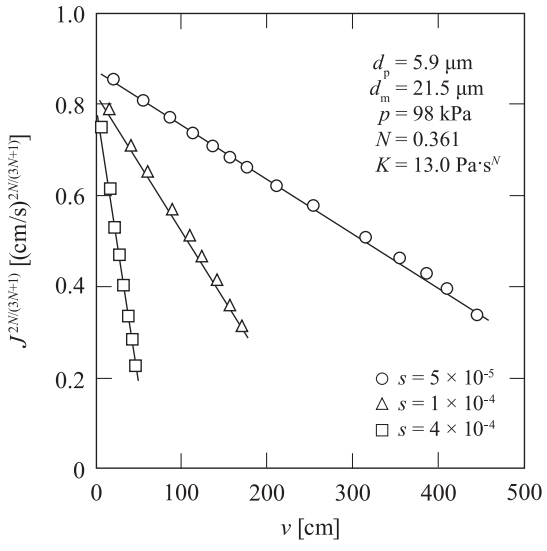

Fig. 4 Flux decline behaviors in clarification filtration of dilute suspensions prepared by suspending diatomaceous earth in aqueous sodium polyacrylate exhibiting behavior of power-law non-Newtonian fluid.

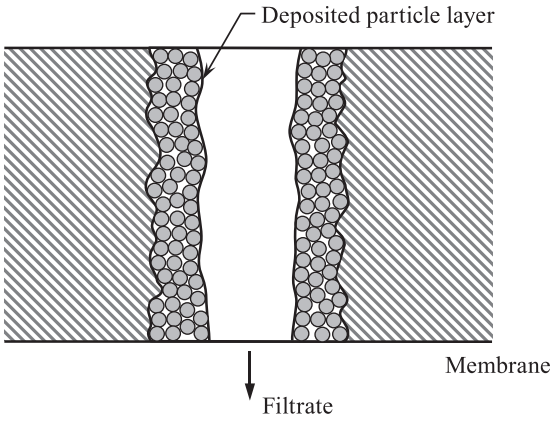

Fig. 5 Schematic view for illustrating the mechanism of membrane fouling in the model presented by Iritani et al. (2007a).

where D_s is the representative diameter of pores on a wetted perimeter basis, D is the representative diameter of pores on a flow cross-sectional area basis, and the subscript 0 indicates the clean membrane. The characteristic form represented by Eq. (17) can be obtained by substituting Eqs. (71) and (72) into Eq. (70) and then by differentiating the reciprocal filtration rate (dt/dv) with respect to v under constant pressure condition ($p = p_0 = \text{const.}$). It should be stressed that Eq. (17) derived in this way is no longer limited by the specific values of n. In this sense, it is concluded that the derivation of Eq. (17) based on the Kozeny-Carman equation is more universal than the classical blocking filtration laws. In a similar way, Eq. (36) applicable to constant rate filtration can be derived based on the Kozeny-Carman equation (Iritani et al., 2011). Some researches were conducted on pore fouling behaviors by employing the Kozeny-Carman equation (Broeckmann et al., 2006; Zhong et al., 2011; Wu et al., 2012). Cheng et al. (2011) derived the characteristic form described by Eq. (17) based on not the Kozeny-Carman equation but the Hagen-Poiseuille equation.

In the derivation of Eq. (17), it is implicitly assumed that the particles are in complete retention, or that the amount of particles deposited within the pores of the membrane increases linearly with v. However, in practice, there often exists some solid leakage through the membrane (Iritani et al., 1994; Rodgers et al., 1995; Hwang et al., 2006; Hwang and Sz, 2010; Polyakov, 2008; Polyakov and Zydney, 2013). As a result, the sieving coefficient of solids varies during the course of filtration. Therefore, the characteristic form represented by Eq. (17) can be generalized by accounting for the variation with time of the amount of the particle deposition within the pores of the membrane. By employing the mass σ of particles deposited on the pore wall per unit membrane area, referred to as the specific deposit (Maroudas and Eisenklam, 1965; Ives and Pienvichitr, 1965; Tien and Payatakes, 1979; Choo and Tien, 1995), the variations of ε and S with the progress of filtration can be, respectively, represented by

$$\varepsilon = \varepsilon_0 - K_m\sigma = \left(1 - \frac{K_m\sigma}{\varepsilon_0}\right)\varepsilon_0 \tag{74}$$

$$S^2(1-\varepsilon)^2 = \left(1 - \frac{K_m\sigma}{\varepsilon_0}\right)^{\beta} S_0^2(1-\varepsilon_0)^2 \tag{75}$$

where K_m is a constant. In a similar way to the derivation of Eq. (17), on the basis of Eq. (70), (74), and (75), the modified form of Eq. (17) can be derived as (Iritani et al., 2010)

$$\frac{d(dt/dv)}{d\sigma} = k\left(\frac{dt}{dv}\right)^n \tag{76}$$

Therefore, when the relation between σ and v is experimentally obtained, the left-hand side value of Eq. (76) may be calculated from the stepwise difference quotient using the experimental data of dt/dv vs. v with the aid of the relation between σ and v. Consequently, the values of n and k in Eq. (76) can be easily obtained from the double logarithmic plots of $d(dt/dv)/d\sigma$ vs. dt/dv.

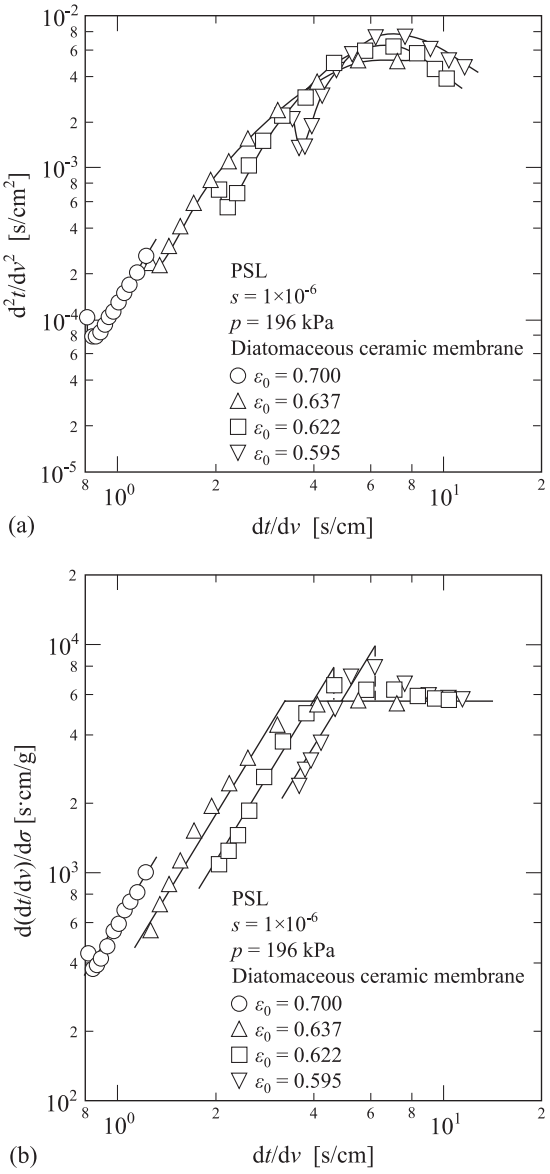

Fig. 6 Characteristic filtration curves for blocking filtration of dilute suspensions of PSL under constant pressure condition using diatomaceous ceramic membranes which are semi-permeable to PSL: (a) logarithmic plots of d^2t/dv^2 vs. dt/dv and (b) logarithmic plots of $d(dt/dv)/d\sigma$ vs. dt/dv.

Fig. 6 compares the logarithmic plots of d^2t/dv^2 vs. dt/dv with those of $d(dt/dv)/d\sigma$ vs. dt/dv for the experimental results in membrane filtration of dilute suspensions of monodisperse polystyrene latex (PSL) under the constant pressure condition using diatomaceous ceramic membranes which are semi-permeable to the PSL (Iritani et al., 2010). The plots for each run show a convex curve with the exception of the case when the initial porosity ε_0

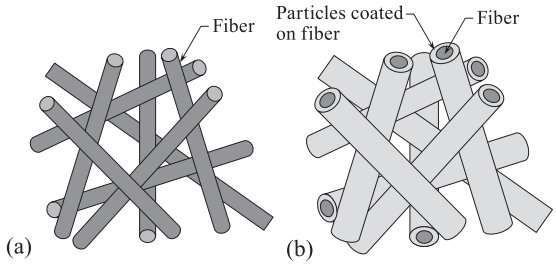

Fig. 7 Schematic view for illustrating the mechanism of membrane fouling in the fiber-coating model presented by Bolton et al. (2005): (a) clean fibers and (b) fouled fibers.

of the membrane is 0.7. The slope of curve gradually decreases with the increase in dt/dv in accordance with the progress of filtration. In contrast, the plots of d(dt/dv)/dσ vs. dt/dv show a linear relation with the same slope of 2.35 for each initial porosity except for the last part of filtration. Thus, Eq. (76) provides a much better description of blocking filtration behaviors obtained for semi-permeable membranes than Eq. (17).

On the basis of the Kozeny-Carman equation, Bolton et al. (2005) proposed a fiber-coating model in which the filter medium becomes plugged as solids coat the surface of cylindrical fibers that constitutes the filter medium. In the model, the fibers become thicker with the progress of filtration, as shown in **Fig. 7**. As a result, the effective radius of fibers increases with time, and correspondingly the porosity decreases, reducing the filter permeability. Therefore, with the aid of the Kozeny-Carman equation, the relation between the filtration rate J and v becomes

$$J = \frac{\mathrm{d}v}{\mathrm{d}t} = \frac{(1 - K_\mathrm{f} v)^3}{\left(1 + \dfrac{\varepsilon_0}{1-\varepsilon_0} K_\mathrm{f} v\right)} J_0 \tag{77}$$

where K_f is the fiber coating constant and equal to the inverse of the solution volume filtered until the filter void volume is completely filled with solids.

2.5 Evaluation of degree of membrane fouling

It is essential to evaluate the degree of membrane fouling during filtration on the basis of the theoretical background in the design of new filter equipment and optimization of commercial filtration operations. The maximum filtrate volume v_max per unit membrane area is defined as the value of v obtained by the time when the filtration rate drops to zero. If the flux decline behavior is controlled by the standard blocking law, on the basis of Eq. (24), v_max can be given as (Badmington et al., 1995; van Reis and Zydney, 2007)

$$v_\mathrm{max} = \frac{2}{K_\mathrm{s}} \tag{78}$$

Combining Eq. (78) with Eq. (24) yields

$$\frac{v}{v_\mathrm{max}} = 1 - \left(\frac{J}{J_0}\right)^{0.5} \tag{79}$$

Consequently, one can evaluate what percentage of v_max has been already obtained when the filtration rate ratio (J/J_0) is known. On the basis of Eqs. (10) and (11), the thickness Δr of the layer deposited on the pore wall is given by (Zeman, 1983; Bowen and Gan, 1991; Blanpain-Avet et al., 1999; Persson et al., 2003)

$$\frac{\Delta r}{r_0} = 1 - \left(\frac{J}{J_0}\right)^{0.25} \tag{80}$$

Similarly to the derivation of Eq. (78), v_max for complete blocking law is written as

$$v_\mathrm{max} = \frac{J_0}{K_\mathrm{b}} \tag{81}$$

Although infinite time is required until the filtration rate becomes zero for intermediate blocking and cake filtration laws, it is possible to calculate the filtrate volume per unit membrane area at an arbitrary ratio (J/J_0) of the flux decline. For instance, when the filtration rate J decreases to y percent of the initial filtration rate J_0, influenced by the intermediate blocking law, the filtrate volume v_y per unit membrane area can be obtained based on Eq. (27) and is represented as

$$v_y = \frac{\ln\left(\dfrac{y}{100}\right)}{K_\mathrm{i}} \tag{82}$$

For the cake filtration law, on the basis of Eq. (30), v_y can be written as

$$v_y = \frac{100 - y}{y K_\mathrm{c} J_0} \tag{83}$$

Fouling index (FI) such as the silt density index (SDI) has been employed to predict and evaluate the fouling potential of the feed water in membrane filtration. The SDI is the most widely applied method for many decades (Nagel, 1987; Yiantsios and Karabelas, 2003; Alhadidi et al., 2011a, 2011b; Koo et al., 2012). According to the ASTM standard (2007), the filtration test is performed under the constant pressure condition of 207 kPa (30 psi) using a microfiltration membrane with the pore size of 0.45 μm. Both the time t_1 required to collect the first 500 ml and the time t_2 required to collect the second 500 ml after 15 min are measured to obtain SDI. Based on the time ratio (t_1/t_2), SDI is calculated as

$$SDI = \frac{100}{15}\left(1 - \frac{t_1}{t_2}\right) \tag{84}$$

SDI values less than 1.0 and 4–5 are preferable for hollow fiber and spiral wound reverse osmosis membranes, respectively. In spite of the widespread application of SDI, it has been long thought that SDI lacks a theoretical basis and that it makes no distinction between different filtration mechanisms. In response to this criticism, White (1996) first clarified the theoretical background based on the cake filtration model. In this case, SDI is written by

$$SDI = \frac{50K_v}{{v_m}^2} \tag{85}$$

More recently, the relation between SDI and blocking filtration laws has been examined in detail for four types of blocking filtration laws consisted of complete blocking, intermediate blocking, standard blocking, and cake filtration (Matsumoto et al., 2009; Alhadidi et al., 2011a; Wei et al., 2012).

The modified fouling index (MFI) proposed by Schippers et al. (1981) was also developed to measure the fouling potential of feed water in membrane filtration. While the feed water is filtered under the constant pressure condition through a 0.45 μm microfiltration membrane in dead-end mode, as is the case in SDI, the filtrate volume is recorded every 30 seconds over the filtration period in the MFI measurement. On the basis of cake filtration model, integrating Eq. (15) under the initial condition that $v = 0$ at $t = 0$, one obtains

$$\frac{t}{v} = (MFI)v + \frac{2}{K_v}v_m \tag{86}$$

Consequently, MFI is the reciprocal of the Ruth coefficient K_v in constant pressure filtration appeared in Eq. (15). Thus, MFI is calculated from the slope obtained by the linear approximation to the plot of the reciprocal average filtration rate (t/v) vs. the filtrate volume v per unit membrane area (Keskinler et al., 2004; Srisukphun et al., 2009). This means that MFI is defined on the assumption that the separation mechanism is controlled by cake filtration. Since MFI includes the solid concentration s in feed water (Park et al., 2006), it is more convenient than the average specific filtration resistance α_{av} to evaluate the fouling potential of feed water in which the solid concentration is unknown. In order to evaluate the fouling potential of smaller colloidal particles or macromolecules, MFI was developed by using ultrafiltration membranes and nanofiltration membranes (referred to as MFI-UF (Boerlage et al., 2002, 2003, 2004) and MFI-NF (Khirani et al., 2006), respectively). Jin et al. (2015) proposed the cake fouling index (CFI) in which the true fouling cake layer resistance can be accurately evaluated by eliminating the effect of pore blocking.

3. Combined model based on blocking filtration law

3.1 Developments of consecutive combined model

Classical blocking filtration laws comprise of three pore blocking mechanisms and a cake formation mechanism. In the generality of cases, the membrane fouling proceeds in two steps: the initial membrane fouling caused by pore blockage and/or pore constriction followed by the long-term fouling arising from the filter cake gradually accumulating on the membrane surface (Kim et al., 1993; Tracey and Davis, 1994; Madaeni and Fane, 1996; Huang and Morrissey, 1998; Blanpain-Avet et al., 1999; Altman et al., 1999; Lim and Bai, 2003; Purkait et al., 2004, 2005; Wang and Tarabara, 2008; Juang et al., 2010; Mohd Amin et al., 2010; Ozdemir et al., 2012). The initial pore blocking frequently causes the irreversible fouling of membranes, resulting in the decrease in the efficiency of membrane cleaning. Once a sufficient fraction of the pores becomes clogged depending on the retentiveness of the membrane, an external cake begins to form on the fouled membrane.

In **Fig. 8**, the logarithmic plots of d^2t/dv^2 as a function of dt/dv are shown as the characteristic filtration curves for filtration of pond water in which the turbidity and concentration of suspended solids are 19.4 NTU and 18.0 mg/l, respectively (Iritani et al., 2007a). In the first stage of filtration (i.e., small dt/dv), the plots show a unique linear relationship, irrespective of the applied filtration pressure p. As filtration proceeds, the reciprocal filtration rate (dt/dv) increases and thus its derivative (d^2t/dv^2) increases. Once the value of d^2t/dv^2 reaches the limiting value, which depends on the filtration pressure, the second stage

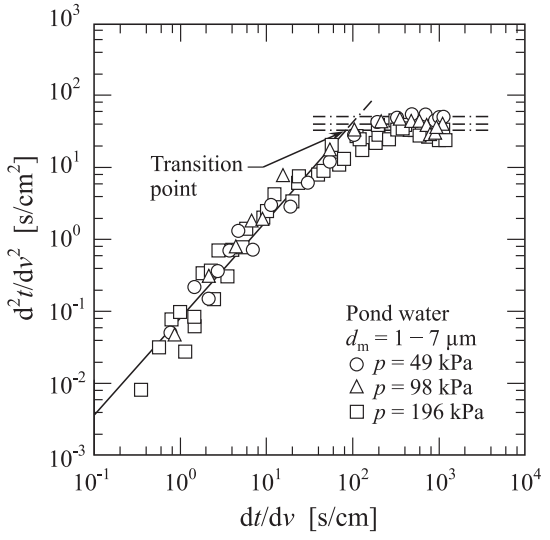

Fig. 8 Characteristic filtration curves for constant pressure filtration of pond water.

begins and the value of d^2t/dv^2 remains constant, as given by Eq. (16). Therefore, the transition point from the initial pore blocking to the following cake filtration during a filtration run can be determined from the change of the slope of the straight line in the double logarithmic plot of d^2t/dv^2 vs. dt/dv according to Eq. (17). It should be noted that the pore fouling is frequently represented by the pore constriction described by the standard blocking law followed by the pore plugging described by the complete or intermediate blocking law (Herrero et al., 1997; Griffiths et al., 2014).

The pore blockage and cake formation may be treated as two resistances in series. According to the resistance-in-series model based on Darcy's law, the filtration rate J is related to the filtration resistances in series as (Iritani et al., 2007b)

$$J = \frac{dv}{dt} = \frac{p}{\mu R} = \frac{p}{\mu(R_m + R_c)} \tag{87}$$

where R is the overall filtration resistance, and R_c is the filter cake resistance. It should be noted that R_m indicates not the resistance of clean membrane but the resistance of fouled membrane.

Bowen et al. (1995) and Iritani et al. (1995) found that the value of n in Eq. (17) gradually varied with the course of filtration in constant pressure dead-end microfiltration of bovine serum albumin (BSA) solution. Later, Hwang et al. (2007) reported a similar result in constant pressure dead-end microfiltration of particulate suspension. In their study, complete blocking ($n = 2$) initially occurred, then gradually changed to standard blocking ($n = 1.5$), and finally cake filtration ($n = 0$) started (Hwang and Chiu, 2008). Therefore, the values of n successively decreased with the progress of filtration.

It should be stressed that several researchers (Bowen et al., 1995; Iritani et al., 1995; Costa et al., 2006; Kim et al., 2007, Yukseler et al., 2007) reported the negative values of n in the later stages of filtration. **Fig. 9** shows the logarithmic plots of d^2t/dv^2 vs. dt/dv as the characteristic form of blocking filtration described by Eq. (17) for constant pressure microfiltration of BSA solution (Iritani et al., 1995). The curve shows a convex shape. The slope of the curve decreases with the increase in dt/dv due to the progress of filtration. Eventually, the slope of the curve has negative values after the slope reaches zero.

Strictly speaking, the blocking filtration laws can be applied only to unstirred dead-end filtration. It is impossible to apply the blocking filtration laws to crossflow filtration where the filter cake growth is restricted by external crossflow of the feed suspension. However, at the earlier stage of crossflow filtration where the solids deposited inside the pore structure, the blocking filtration laws are frequently employed to describe the progressive pore clogging. For instance, Murase and Ohn (1996) adopted

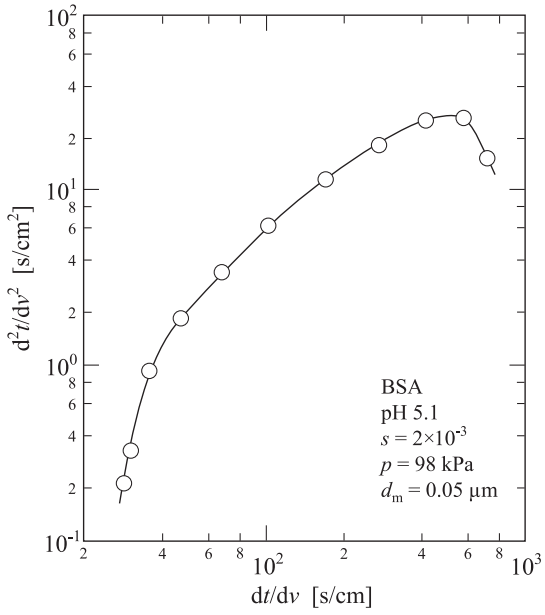

Fig. 9 Characteristic filtration curve for constant pressure microfiltration of BSA solution.

the intermediate blocking law to describe the membrane fouling behavior in the initial stage of crossflow microfiltration of polymethyl methacrylate (PMMA) suspension.

The blocking filtration law has been frequently employed in the analysis of the flux decline in crossflow filtration (Jonsson et al., 1996; Prádanos et al., 1996; Keskinler et al., 2004). In this case, the flux decline behaviors should be analyzed by introducing the term of a steady-state flux controlled by crossflow (Field et al., 1995; de Bruijn et al., 2005). Field et al. (1995) modified the blocking filtration equation (18) by accounting for the back-transport effect arising from crossflow as

$$\frac{dJ}{dt} = -k(J - J_{lim})J^{2-n} \tag{88}$$

where J_{lim} is the critical filtration rate under steady-state condition. Equation (88) has been widely employed in the analysis of the flux decline behaviors in crossflow membrane filtration of a variety of colloids (Todisco et al., 1996; Blanpain and Lalande, 1997; de Barros et al., 2003; Rai et al., 2006; Cassano et al., 2007; Mondal and De, 2009; Vera et al., 2009; Ma et al., 2010; Chang et al., 2011; Daniel et al., 2011; Field and Wu, 2011; Huang et al., 2014). Electric field-assisted membrane filtration in which the particle deposition was restricted due to an external electric field was also investigated on the basis of blocking filtration laws as well as crossflow membrane filtration (Sarkar and De, 2012).

3.2 Developments of concurrent combined model

While membrane fouling generally proceeds in two

steps consisted of pore blocking followed by cake formation, as mentioned above, pore blocking and cake formation may be frequently occurring simultaneously during the filtration process (Takahashi et al., 1991; Matsumoto et al., 1992; Katsoufidou et al., 2005; Fernández et al., 2011; Li et al., 2011; Nakamura et al., 2012). Bolton et al. (2006a) combined two blocking filtration laws occurring concurrently among four blocking filtration laws. On the basis of the Darcy's law, the volumetric flow rate Q through the membrane is related to the overall filtration resistance R and the effective filtration area A in the form

$$Q = \frac{A}{R} \cdot \frac{p}{\mu} \tag{89}$$

Since the apparent filtration area remains constant during the course of filtration, the filtration rate J (= dv/dt) is directly proportional to the volumetric flow rate Q in Eq. (89) as

$$\frac{J}{J_0} = \frac{Q}{Q_0} \tag{90}$$

where the subscript "0" indicates the value at the start of filtration. Substituting Eq. (89) into Eq. (90), one obtains

$$\frac{J}{J_0} = \frac{R_0 A}{R A_0} \tag{91}$$

Both complete and intermediate blocking mechanisms contribute the decrease in the effective filtration area A. In contrast, both standard blocking and cake filtration mechanisms increase the filtration resistance R. On the basis of Eqs. (21) and (27), the variations of the effective filtration area A in Eq. (91) for complete and intermediate blocking mechanisms are, respectively, represented as

$$\frac{A}{A_0} = 1 - \frac{K'_b}{J_0} V \tag{92}$$

$$\frac{A}{A_0} = \exp(-K'_i V) \tag{93}$$

where K'_b and K'_i are the blocking constants for complete and intermediate blocking laws, respectively, and V is the filtrate volume. On the basis of Eq. (24) and (30), the variations of the filtration resistance R in Eq. (91) for standard blocking and cake filtration models are, respectively, given in

$$R = R_0 \left(1 - \frac{K'_s V}{2}\right)^{-2} \tag{94}$$

$$R = R_0 (1 + K'_c J_0 V) \tag{95}$$

where K'_s and K'_c are the blocking constants for standard blocking and cake filtration laws, respectively. Consequently, for instance, the governing equation for the combined process in which both intermediate blocking and cake formation occur simultaneously is derived using Eqs. (91), (93), and (95) and is given by

$$\frac{J}{J_0} = (\exp(-K'_i V))(1 + K'_c J_0 V)^{-1} \tag{96}$$

Just around the same time, Duclos-Orsello et al. (2006) also proposed a very similar combined model for describing the membrane fouling. Rezaei et al. (2011) employed the combined model developed by Bolton et al. (2006a) to analyze the fouling mechanism in crossflow microfiltration of whey. Affandy et al. (2013) well described fouling behaviors in sterile microfiltration of large plasmids DNA with the use of the standard—intermediate model.

Bolton et al. (2006b) combined the adsorption model with the classical blocking filtration model by a method similar to that mentioned above. In the adsorption model, it is assumed that foulant adsorption occurs at the pore walls with zeroth-order kinetics, thereby reducing the pore size and thus increasing the filtration resistance. As a result, the increase in the resistance R with filtration time t is written as

$$\frac{R_0}{R} = (1 - K_a t)^4 \tag{97}$$

where K_a is the adsorption blocking constant. Consequently, for instant, in a combined intermediate blocking—adsorption model, substituting Eqs. (93) and (97) into Eq. (91), one gets

$$\frac{J}{J_0} = \exp(-K_i V)(1 - K_a t)^4 \tag{98}$$

Integration of Eq. (98) lead to the relation between V and t in the form:

$$V = \frac{1}{K_i} \ln\left(\frac{K_i J_0}{5K_a}\left\{1 - (1 - K_a t)^5\right\} + 1\right) \tag{99}$$

Giglia and Straeffer (2012) applied the combined intermediate blocking—adsorption model to the evaluation of filtration performance of microfiltration membranes operated in series. The combined cake—adsorption model can be described by adding the filtration resistances due to the adsorption and cake formation as

$$\frac{J}{J_0} = \left\{(1 - K_a t)^{-4} + K_c J_0 V\right\}^{-1} \tag{100}$$

In the initial stage of cake filtration, pore blocking of a membrane often occurs. As a result, the membrane resistance gradually increases with time and approaches to the saturated value, as indicated by Notebaert et al. (1975). On the assumption that the membrane resistance approaches a finite value due to the progress of filtration, the following equation was presented for describing the variation of the clogged membrane resistance R_m during the

course of filtration for cake filtration of liquefied coal (Tiller et al., 1981; Leu and Tiller, 1983).

$$\frac{R_m - R_{m0}}{R_{m\infty} - R_{m0}} = 1 - \exp(-\eta w) \tag{101}$$

where R_{m0} and $R_{m\infty}$ are the initial and infinite membrane resistances, respectively, η is the blocking rate constant, and w is the net solid mass in the filter cake per unit membrane area. Thereafter, Lee (1997) developed a more rigorous model by introducing the intermediate blocking law and derived the equation with two fitting parameters as

$$\frac{R_m - R_{m0}}{R_{m\infty} - R_{m0}} = \frac{1 - \exp(-\eta w)}{1 + \lambda \exp(-\eta w)} \tag{102}$$

where λ is a constant. Interestingly, Eq. (102) reduces to Eq. (101) found experimentally by Tiller et al. (1981) when the membrane clogging is quite-serious, i.e., at the limit $\lambda \to 0$.

By imposing the condition that some of pores of the membrane still remain open finally in the intermediate blocking law, Iritani et al. (2005) described the clogged membrane resistance R_m as

$$\frac{1 - \dfrac{R_{m0}}{R_m}}{1 - \dfrac{R_{m0}}{R_{m\infty}}} = 1 - \exp(-\eta w) \tag{103}$$

It should be noted that the variation of R_m with w can be represented by only one fitting parameter η in Eq. (103) while two fitting parameters η and λ are required in the analysis of pore clogging using Eq. (102). The cake resistance R_c is related to w as

$$R_c = \alpha_{av} w \tag{104}$$

Thus, the increasing behaviors of filtration resistance can be described by adding the cake resistance R_c represented by Eq. (104) to clogged membrane resistance R_m represented by Eq. (103) on the basis of Eq. (87) describing the resistance-in-series model. In this case, all the particles retained by the membrane contribute as the cake resistance R_c and a part of them also serve as the clogged membrane resistance R_m by clogging the membrane pores in accordance with the intermediate blocking law considering the limiting value of the clogging resistance on the basis of the concurrent combined model, as schematically shown in **Fig. 10**.

Fig. 11 shows the characteristic curves of blocking filtration laws, which is plotted in the form of d^2t/dv^2 vs. dt/dv, for different feed concentrations in constant pressure microfiltration of monodisperse PSL with a particle diameter d_p of 0.522 μm filtered under the applied pressure p of 196 kPa using the track-etched polycarbonate membrane with a nominal pore size d_m of 0.2 μm (Iritani et al., 2015). Each plot results in the distinct negative slope in

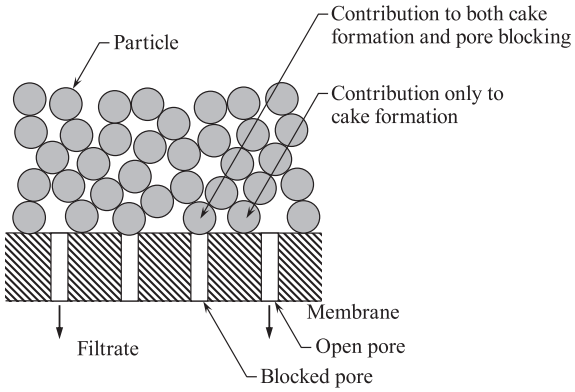

Fig. 10 Schematic view for illustrating the mechanism of membrane fouling comprised of both pore blocking and cake formation occurring simultaneously in the model presented by Iritani et al. (2005).

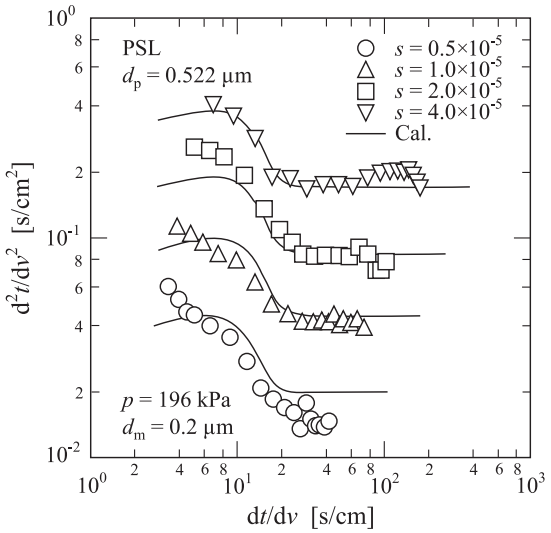

Fig. 11 Effect of solid mass fraction in suspension on characteristic filtration curves in constant pressure microfiltration.

the initial period of filtration since the filtration behaviors are influenced both by the pore blocking of membrane and by cake formation, as reported by several researchers (Bowen et al., 1995; Iritani et al., 1995; Ho and Zydney, 2000; Hwang et al., 2007; Yukseler et al., 2007). However, as filtration proceeds, cake filtration has a dominant influence on the filtration behaviors and thus the slope of the plot becomes equal to zero. Substituting Eqs. (103) and (104) into Eq. (87) and using the relation that $w = \rho s v$ on the assumption that suspension is very dilute, one obtains

$$\frac{dt}{dv} = \frac{\mu}{p}\left(\frac{R_{m\infty}}{1+F} + \alpha_{av}\rho s v\right) \tag{105}$$

where F is a function defined by

$$F = \frac{R_{m\infty} - R_{m0}}{R_{m0}} \exp(-\eta \rho s v) \tag{106}$$

Subsequently, differentiating Eq. (105) with respect to v under constant pressure condition, one gets

$$\frac{\mathrm{d}^2 t}{\mathrm{d}v^2} = \frac{\mu\rho s}{p}\left(\frac{\eta F}{(1+F)^2} + \alpha_{\mathrm{av}}\right) \tag{107}$$

Therefore, the curve of $\mathrm{d}^2t/\mathrm{d}v^2$ vs. $\mathrm{d}t/\mathrm{d}v$ can be evaluated from Eq. (107) with the aid of Eq. (105). The solid curves in **Fig. 11** are the calculations and it is of significance to note that the calculations roughly reflect the trends of experimental data, indicating the negative slope in the initial period followed by the straight line with the slope of zero.

Hwang et al. (2006) evaluated the protein capture into the interstices of filter cake in crossflow microfiltration of particle/protein binary mixtures on the basis of the deep-bed filtration mechanism. The apparent protein rejection R_{obs} is evaluated from

$$R_{\mathrm{obs}} = 1 - \frac{C_{\mathrm{p}}}{C_{\mathrm{b}}} = 1 - \exp(-\gamma L_{\mathrm{c}}) \tag{108}$$

where C_{p} and C_{b} are protein concentrations in the filtrate and in the bulk feed suspension, respectively, γ is a screening parameter which represents the protein fraction rejected by the filter cake per unit cake thickness, and L_{c} is the thickness of the filter cake.

Ho and Zydney (2000) presented a unique model describing pore blocking and cake formation occurring simultaneously in microfiltration processes. As schematically shown in **Fig. 12**, the filter cake only forms over the regions of the membrane which have already been blocked by the initial deposit in the membrane pores. This means that the pore blockage did not lead to complete loss of flow through the pore. As a result, according to Darcy's law, the flux J_{blocked} through the already blocked pores can be written as

$$J_{\mathrm{blocked}} = \frac{p}{\mu(R_{\mathrm{m0}} + R_{\mathrm{c}})} \tag{109}$$

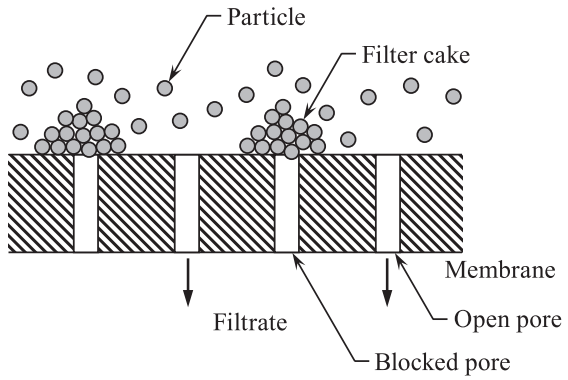

Fig. 12 Schematic view for illustrating the mechanism of membrane fouling comprised of both pore blocking and cake formation occurring simultaneously in the model presented by Ho and Zydney (2000).

The cake resistance R_{c} increases with time during the course of filtration as

$$\frac{\mathrm{d}R_{\mathrm{c}}}{\mathrm{d}t} = f'\alpha_{\mathrm{av}} J_{\mathrm{blocked}} C_{\mathrm{b}} \tag{110}$$

where f' is the fraction of solutes which contribute to the growth of filter cake. Integrating Eq. (110) with the aid of Eq. (109), one obtains

$$R_{\mathrm{c}} = (R_{\mathrm{m0}} + R_{\mathrm{c0}})\sqrt{1 + \frac{2f'\alpha_{\mathrm{av}} p C_{\mathrm{b}} t}{\mu(R_{\mathrm{m0}} + R_{\mathrm{c0}})^2}} - R_{\mathrm{m0}} \tag{111}$$

where R_{c0} is the flow resistance of the first cake layer. The filtration rate J can be given as the sum of the flow rate through open and blocked pores. Thus, with the use of Eq. (111), the variation of J with t can be approximately written as

$$\frac{J}{J_0} = \exp\left(-\frac{\alpha p C_{\mathrm{b}}}{\mu R_{\mathrm{m0}}} t\right) + \frac{R_{\mathrm{m0}}}{R_{\mathrm{m0}} + R_{\mathrm{c}}}\left\{1 - \exp\left(-\frac{\alpha p C_{\mathrm{b}}}{\mu R_{\mathrm{m0}}} t\right)\right\} \tag{112}$$

where α is the pore blocking constant in the complete blocking law. The first term in Eq. (112) represents a simple exponential decline in the flux through the open pores controlled by the classical complete blocking law. As filtration proceeds, the deposit continued to grow due to some fluid flow through pores partially blocked by the complete blocking mechanism, as illustrated by **Fig. 12**, and thus the filtration rate becomes governed by the classical cake filtration law represented by the second term in Eq. (112). The model has been extensively used to analyze the fouling behaviors in membrane filtration of a number of colloids under various operating conditions (Yuan et al., 2002; Ho and Zydney, 2002; Palacio et al., 2002, 2003; Taniguchi et al., 2003; Ye et al., 2005; Chandler and Zydney, 2006; Cogan and Chellam, 2009; Byun et al., 2011).

4. Conclusions and prospective view

The present article overviewed the blocking filtration laws comprised of the complete blocking, standard blocking, intermediate blocking, and cake filtration, which could describe the increase in the filtration resistance during the course of filtration in membrane filtration of colloids. The equations derived based on the blocking filtration laws were reported to describe the filtrate flow of Newtonian and non-Newtonian fluids through membranes for both constant pressure and constant rate filtration processes. The blocking filtration laws are quite useful due to the simplicity in use of the model to identify the prevailing fouling mechanism from the experimental data of the flux decline in constant pressure filtration or pressure rise in constant rate filtration. In order to evaluate more com-

plicate fouling behaviors in membrane filtration, several combined models have been developed based on the blocking filtration laws and well described the fouling phenomena in which more than one filtration mechanism occurred successively or simultaneously.

While the blocking filtration laws and their combinations largely contributed to the optimal choice of the membrane and membrane-cleaning strategy in industrial use, it is essential to develop more sophisticated models which can describe more accurately the complicated behaviors of membrane fouling actually encountered in industrial membrane filtration. In particular, there is a pressing need for developing the models which are applicable not only the simple model colloids but also to the actual colloids containing a wide variety of ingredients, as frequently encountered in water treatment.

In any case, the elucidation of mechanism predominating the membrane fouling in membrane filtration is ever lasting problems crying out for solutions. We believe that this article provides a valuable insight into the further developments of models which can reasonably describe the fouling behaviors in membrane filtration.

Acknowledgements

This work has been partially supported by Grant-in-Aid for Scientific Research from The Ministry of Education, Culture, Sports, Science and Technology, Japan. The authors wish to acknowledge with sincere gratitude the financial support leading to the publication of this article.

Nomenclature

A	effective filtration area (m^2)
A_0	initial effective filtration area (m^2)
a	constant in Eq. (33)
C_b	protein concentration in bulk feed suspension (kg/m^3)
C_p	protein concentration in filtrate (kg/m^3)
c	volume of particles trapped per unit filtrate volume v per unit membrane area (m)
D	representative diameter of pores on flow cross-sectional area basis (m)
D_s	representative diameter of pores on wetted perimeter basis (m)
d_m	pore size (m)
d_p	diameter of suspended solids (m)
F	function defined by Eq. (106)
f'	fraction of solutes which contribute to growth of filter cake
J	filtration rate (m/s)
J_0	initial filtration rate (m/s)
$J_{blocked}$	flux through already blocked pores (m/s)
J_{lim}	critical filtration rate under steady-state condition in crossflow filtration (m/s)
K	fluid consistency index for power-law non-Newtonian fluids ($kg\ m^{-1}\ s^{N-2}$)
K_a	adsorption blocking constant in Eq. (97) (s^{-1})
K_b	blocking constant in Eq. (2) for complete blocking law (s^{-1})
K'_b	blocking constant in Eq. (92) for complete blocking law ($m^{-2}\ s^{-1}$)
K_{br}	blocking constant in Eq. (35) for complete blocking law in constant rate filtation ($kg^{-1}\ s^2$)
K_c	blocking constant in Eq. (16) for cake filtration law (s/m^2)
K'_c	blocking constant in Eq. (95) for cake filtration law (s/m^4)
K_f	fiber coating constant in Eq. (77)
K_i	blocking constant in Eq. (3) for intermediate blocking law (m^{-1})
K'_i	blocking constant in Eq. (93) for intermediate blocking law (m^{-3})
K_m	constant in Eq. (74) (m^2/kg)
K_p	constant in Eq. (71) (m^{-1})
K_s	blocking constant in Eq. (7) for standard blocking law (m^{-1})
K'_s	blocking constant in Eq. (94) for standard blocking law (m^{-3})
K_v	Ruth coefficient in constant pressure cake filtration (m^2/s)
k	resistant coefficient in Eq.(17) ($m^{n-2}\ s^{1-n}$)
k'	resistant coefficient in Eq. (36) for constant rate filtration ($kg^{1-n'}\ m^{n'-2}\ s^{2n'-2}$)
k_0	Kozeny constant
k_1	constant in Eq. (44) ($kg^{1-n_1}\ m^{n_1-2}\ s^{2n_1-2}$)
k'_1	constant in Eq. (46) ($kg^{n'_1-2}\ m^{2-2n'_1}\ s^{5-5n'_1}$)
k_2	constant in Eq. (45) ($kg^{1-n'}\ m^{n'-1}\ s^{2n'-3}$)
k'_2	constant in Eq. (47) ($kg^{1-n'_2}\ m^{2n'_2-3}\ s^{2n'_2-2}$)
k_c	proportional constant in Eq. (1) ($kg^{-1}\ m^4\ s$)
k_j	constant in Eq. (31) (s^{-1})
k_N	constant in Eq. (58) ($m^{n_N-2}s^{1-n_N}$)
k'_N	constant in Eq. (59) ($kg^{1-n'_N}\ m^{n'_N-2}\ s^{2n'_N-2}$)
L	membrane thickness (m)
L_c	thickness of filter cake (m)
m	ratio of mass of wet to mass of dry cake
MFI	modified fouling index defined by Eq. (86) (s/m^2)

N fluid behavior index for power-law non-Newtonian fluids

N' number of open pores per unit effective membrane area at filtrate volume v per unit effective membrane area (m^{-2})

N'_0 total number of open pores per unit effective membrane area at start of filtration (m^{-2})

n blocking index in Eq. (17)

n' blocking index in Eq. (36) for constant rate filtration

n_1 compressibility coefficient in Eq. (42)

n'_1 constant in Eq. (46)

n'_2 constant in Eq. (47)

n_j constant in Eq. (31)

n_N constant in Eq. (58)

n'_N constant in Eq. (59)

p applied filtration pressure (Pa)

p_0 initial applied filtration pressure (Pa)

Q volumetric flow rate (m^3/s)

Q_0 initial volumetric flow rate (m^3/s)

R overall filtration resistance (m^{-1})

R_0 initial overall filtration resistance (m^{-1})

R_c filter cake resistance (m^{-1})

R_{c0} flow resistance of the first cake layer (m^{-1})

R_m clogged membrane resistance (m^{-1})

R_{m0} initial membrane resistance (m^{-1})

$R_{m\infty}$ infinite membrane resistance (m^{-1})

r pore radius (m)

r_0 initial pore radius (m)

S specific surface area of membrane (m^{-1})

S_0 initial specific surface area of clean membrane (m^{-1})

S_c constant in Eq. (33)

s mass fraction of solids in colloids

SDI silt density index defined by Eq. (84)

t filtration time (s)

t_1 time required to collect the first 500 ml of filtrate volume (s)

t_2 time required to collect the second 500 ml of filtrate volume after 15 min (s)

u average flow rate (m/s)

V filtrate volume (m^3)

v filtrate volume per unit effective membrane area (m)

v_m fictitious filtrate volume per unit membrane area required to obtain cake with flow resistance equivalent to that of membrane (m)

v_{max} maximum filtrate volume per unit membrane area (m)

v_y filtrate volume per unit membrane area obtained until filtration rate decreases to y percent of initial filtration rate (m)

w net solid mass in filter cake per unit membrane area (kg/m^2)

x number of particles blocking pores per unit filtrate volume (m^{-3})

y percentage of initial value of filtration rate

α pore blocking constant in Eq. (112) for complete blocking law (m^2/kg)

α_0 average specific cake resistance at null stress in Eq. (48) (m/kg)

α_1 constant in Eq. (42) ($kg^{-1-n_1} m^{1+n_1} s^{2n_1}$)

α_2 constant in Eq. (48) ($kg^{-2} m^2 s^2$)

α_{av} average specific cake resistance (m/kg)

β constant which depends on mode of morphology of deposit assemblages

γ screening parameter in Eq. (108) (m^{-1})

$\dot{\gamma}$ shear rate (s^{-1})

γ_{av} average specific cake resistance for power-law non-Newtonian flow (m^{2-N}/kg)

Δr thickness of layer deposited on pore wall (m)

ε porosity of membrane

ε_0 initial porosity of clean membrane

ε_p packing porosity of particle layer formed on pore wall

η blocking rate constant (m^2/kg)

λ constant in Eq. (102)

μ viscosity of filtrate (Pa s)

ρ density of filtrate (kg/m^3)

σ specific deposit, i.e., mass of particles deposited on pore wall per unit membrane area (kg/m^2)

τ shear stress (Pa)

References

Affandy A., Keshavarz-Moore E., Versteeg H.K., Application of filtration blocking models to describe fouling and transmission of large plasmids DNA in sterile filtration, Journal of Membrane Science, 437 (2013) 150–159.

Alhadidi A., Blankert B., Kemperman A.J.B., Schippers J.C., Wessling M., van der Meer W.G.J., Effect of testing conditions and filtration mechanisms on SDI, Journal of Membrane Science, 381 (2011a) 142–151.

Alhadidi A., Kemperman A.J.B., Schippers J.C., Wessling M., van der Meer W.G.J., The influence of membrane properties on the Silt Density Index, Journal of Membrane Science, 384 (2011b) 205–218.

Altman M., Semiat R., Hasson D., Removal of organic foulants from feed waters by dynamic membranes, Desalination, 125 (1999) 65–75.

ASTM Standard (D4189-07), Standard test method for silt density index (SDI) of water, D19.08 on membranes and ion exchange materials, 2007.

Badmington F., Wilkins R., Payne M., Honig E.S., Vmax testing for practical microfiltration train scale-up in biopharmaceutical processing, Pharmaceutical Technology, 19(Sep.) (1995) 64–76.

Blankert B., Betlem B.H.L., Roffel B., Dynamic optimization of a dead-end filtration trajectory: Blocking filtration laws, Journal of Membrane Science, 285 (2006) 90–95.

Blanpain P., Hermia J., Lenoël M., Mechanisms governing permeate flux and protein rejection in the microfiltration of beer with a cyclopore membrane, Journal of Membrane Science, 84 (1993) 37–51.

Blanpain P., Lalande M., Investigation of fouling mechanisms governing permeate flux in the crossflow microfiltration of beer, Filtration & Separation, 21 (1997) 1065–1069.

Blanpain-Avet P., Fillaudeau L., Lalande M., Investigation of mechanisms governing membrane fouling and protein rejection in the sterile microfiltration of beer with an organic membrane, Transactions of The Institution of Chemical Engineers, Part C, Food and Bioproducts Processing, 77 (1999) 75–89.

Boerlage S.F.E., Kennedy M.D., Dickson M.R., El-Hodali D.E.Y., Schippers J.C., The modified fouling index using ultrafiltration membranes (MFI-UF): Characterisation, filtration mechanism and proposed reference membrane, Journal of Membrane Science, 197 (2002) 1–21.

Boerlarge S.F.E., Kennedy M., Aniye M.P., Schippers J.C., Application of the MFI-UF to measure and predict particulate fouling in RO systems, Journal of Membrane Science, 220 (2003) 97–116.

Boerlage S.F.E., Kennedy M., Tarawneh Z., de Feber R., Shippers J.C., Development of the MFI-UF in constant flux filtration, Desalination, 161 (2004) 103–113.

Bolton G.R., LaCasse D., Lazzara M.J., Kuriyel R., The fiber-coating model of biopharmaceutical depth filtration, AIChE Journal, 51 (2005) 2978–2987.

Bolton G.R., Lacasse D., Kuriyel R., Combined models of membrane fouling: Development and application to microfiltration and ultrafiltration of biological fluids, Journal of Membrane Science, 277 (2006a) 75–84.

Bolton G.R., Boesch A.W., Lazzara M.J., The effects of flow rate on membrane capacity: Development and application of adsorptive membrane fouling models, Journal of Membrane Science, 279 (2006b) 625–634.

Bowen W.R., Gan Q., Properties of microfiltration membranes: Flux loss during constant pressure permeation of bovine serum albumin, Biotechnology and Bioengineering, 38 (1991) 687–696.

Bowen W.R., Calvo J.I., Hernández A., Steps of membrane blocking in flux decline during protein microfiltration, Journal of Membrane Science, 101 (1995) 153–165.

Broekmann A., Busch J., Wintgens T., Marquardt W., Modeling of pore blocking and cake layer formation in membrane filtration for wastewater treatment, Desalination, 189 (2006) 97–109.

Byun S., Taurozzi J.S., Alpatova A.L., Wang F., Tarabara V.V., Performance of polymeric membranes treating ozonated surface water: Effect of ozone dosage, Separation and Purification Technology, 81 (2011) 270–278.

Cassano A., Marchio M., Driori E., Clarification of blood orange juice by ultrafiltration: Analyses of operating parameters, membrane fouling and juice quality, Desalination, 212 (2007) 15–27.

Chandler M., Zydney A., Effects of membrane pore geometry on fouling behavior during yeast cell microfiltration, Journal of Membrane Science, 285 (2006) 334–342.

Chang E.E., Yang S.Y., Huang C.P., Liang C.H., Chiang P.C., Assessing the fouling mechanisms of high-pressure nanofiltration membrane using the modified Hermia model and the resistance-in-series model, Separation and Purification Technology, 79 (2011) 329–336.

Chellam S., Xu W., Blocking laws analysis of dead-end constant flux microfiltration of compressible cakes, Journal of Colloid and Interface Science, 301 (2006) 248–257.

Chellam S., Cogan N.G., Colloidal and bacterial fouling during constant flux microfiltration: Comparison of classical blocking laws with a unified model combining pore blocking and EPS secretion, Journal of Membrane Science, 382 (2011) 148–157.

Cheng Y.L., Lee D.J., Lai J.Y., Filtration blocking laws: Revisited, Journal of the Taiwan Institute of Chemical Engineers, 42 (2011) 506–508.

Choo C.U., Tien C., Simulation of hydrosol deposition in granular media, AIChE Journal, 41 (1995) 1426–1442.

Chudacek M.W., Fane A.G., The dynamics of polarization in unstirred and stirred ultrafiltration, Journal of Membrane Science, 21 (1984) 145–160.

Cogan N.G., Chellam S., Incorporating pore blocking, cake filtration, and EPS production in a model for constant pressure bacterial fouling during dead-end microfiltration, Journal of Membrane Science, 345 (2009) 81–89.

Costa A.R., Pinho M.N., Elimelech M., Mechanism of colloidal natural organic matter fouling in ultrafiltration, Journal of Membrane Science, 281 (2006) 716–725.

Daniel R.C., Billing J.M., Russell R.L., Shimskey R.W., Smith H.D., Peterson R.A., Integrated pore blockage – cake filtration model for crossflow filtration, Chemical Engineering Research and Design, 89 (2011) 1094–1103.

de Barros S.T.D., Andrade C.M.G., Mendes E.S., Peres L., Study of fouling mechanism in pineapple juice clarification by ultrafiltration, Journal of Membrane Science, 215 (2003) 213–224.

de Bruijn J.P.F., Salazar F.N., Bórquez R., Membrane blocking in ultrafiltration: A new approach to fouling, Transaction of The Institution of Chemical Engineers, Part C, Food and Bioproducts Processing, 83 (2005) 211–219.

de Lara R., Benavente J., Use of hydrodynamic and electrical measurements to determine protein fouling mechanisms for microfiltration membranes with different structures and materials, Separation and Purification Technology, 66 (2009) 517–524.

Duclos-Orsello C., Li W., Ho C.C., A three mechanism model to describe fouling of microfiltration membranes, Journal of Membrane Science, 280 (2006) 856–866.

Fan L.T., Hwang S.H., Chou S.T., Nassar R., Birth-death modeling of deep bed filtration: Sectional analysis, Chemical Engineering Communications, 35 (1985a) 101–121.

Fan L.T., Nassar R., Hwang S.H., Chou S.T., Analysis of deep bed filtration data: Modeling as a birth-death process, AIChE Journal, 31 (1985b) 1781–1790.

Fane A.G., Fell C.J.D., Suki A., The effect of pH and ionic environment on the ultrafiltration of protein solutions with retentive membranes, Journal of Membrane Science, 16 (1983) 195–210.

Fernández X.R., Rosenthal I., Anlauf H., Nirschl H., Experimental and analytical modeling of the filtration mechanisms of a paper stack candle filter, Chemical Engineering Research and Design, 89 (2011) 2776–2784.

Field R.W., Wu D., Howell J.A., Gupta B.B., Critical flux concept for microfiltration fouling, Journal of Membrane Science, 100 (1995) 259–272.

Field R.W., Wu J.J., Modeling of permeability loss in membrane filtration: Re-examination of fundamental fouling equations and their link to critical flux, Desalination, 283 (2011) 68–74.

Giglia S., Straeffer G., Combined mechanism fouling model and method for optimization of series microfiltration performance, Journal of Membrane Science, 417–418 (2012) 144–153.

Gironès M., Lammertink R.G.L., Wessling M., Protein aggregate deposition and fouling strategies with high-flux silicon nitride microsieves, Journal of Membrane Science, 273 (2006) 68–76.

Grace H.P., Resistance and compressibility of filter cake, Part I, Chemical Engineering Progress, 49 (1953) 303–318.

Grace H.P., Structure and performance of filter media. II. Performance of filter media in liquid service, AIChE Journal, 2 (1956) 316–336.

Granger J., Dodds J., Leclerc D., Filtration of low concentrations of latex particles on membrane filters, Filtration & Separation, 9 (1985) 58–60.

Griffiths I.M., Kumar A., Stewart P.S., A combined network model for membrane fouling, Journal of Colloid and Interface Science, 432 (2014) 10–18.

Heertjes P.M., Studies in filtration, Blocking filtration, Chemical Engineering Science, 6 (1957) 190–203.

Hermans P.H., Bredée H.L., Zur kenntnis der filtrationsgesetze, Recueil des Travaux Chimiques des Pays-Bas, 54 (1935) 680–700.

Hermans P.H., Bredée H.L., Principles of the mathematic treatment of constant-pressure filtration, Journal of The Society of Chemical Industry, 55T (1936) 1–4.

Hermia J., Constant pressure blocking filtration laws—Application to power-law non-Newtonian fluids, Transaction of The Institution of Chemical Engineers, 60 (1982) 183–187.

Herrero C., Prádanos P., Calvo J.I., Tejerina F., Hernández A., Flux decline in protein microfiltration: Influence of operative parameters, Journal of Colloid and Interface Science, 187 (1997) 344–351.

Hlavacek M., Bouchet F., Constant flowrate blocking laws and an example of their application to dead-end microfiltration of protein solutions, Journal of Membrane Science, 82 (1993) 285–295.

Ho C.C., Zydney A.L., Effect of membrane morphology on the initial rate of protein fouling during microfiltration, Journal of Membrane Science, 155 (1999) 261–275.

Ho C.C., Zydney A.L., A combined pore blockage and cake formation model for protein fouling during microfiltration, Journal of Colloid and Interface Science, 232 (2000) 389–399.

Ho C.C., Zydney A.L., Transmembrane pressure profiles during constant flux microfiltration of bovine serum albumin, Journal of Membrane Science, 209 (2002) 363–377.

Hodgson P.H., Leslie G.L., Schneider R.P., Fane A.G., Fell C.J.D., Marshall K.C., Cake resistance and solute rejection in bacterial microfiltration: The role of the extracellular matrix, Journal of Membrane Science, 79 (1993) 35–53.

Hsu E.H., Fan L.T., Experimental study of deep bed filtration: A stochastic treatment, AIChE Journal, 30 (1984) 267–273.

Huang L., Morrissey M.T., Fouling of membranes during microfiltration of surimi wash water: Roles of pore blocking and surface cake filtration, Journal of Membrane Science, 144 (1998) 113–123.

Huang Q., Gomaa H.G., Hashem N., Flux characteristics of oil separation from O/W emulsions using highly hydrophilic UF membrane in narrow channel, Separation Science and Technology, 49 (2014) 12–21.

Hwang K.J., Chou F.Y., Tung K.L., Effects of operating conditions on the performance of cross-flow microfiltration of fine particle/protein binary suspension, Journal of Membrane Science, 274 (2006) 183–191.

Hwang K.J., Liao C.Y., Tung K.L., Analysis of particle fouling during microfiltration by use of blocking models, Journal of Membrane Science, 287 (2007) 287–293.

Hwang K.J., Chiu H.S., Influence of membrane type on filtration characteristics and protein rejection in crossflow microfiltration, Filtration, 8 (2008) 317–322.

Hwang K.J., Sz P.Y., Filtration characteristics and membrane fouling in cross-flow microfiltration of BSA/dextran binary suspension, Journal of Membrane Science, 347 (2010) 75–82.

Iritani E., Nakatsuka S., Aoki H., Murase T., Effect of solution environment on unstirred dead-end ultrafiltration characteristics of proteinaceous solutions, Journal of Chemical Engineering of Japan, 24 (1991a) 177–183.

Iritani E., Sumi H., Murase T., Analysis of filtration rate in clarification filtration of power-law non-Newtonian fluids-solids mixtures under constant pressure by stochastic model, Journal of Chemical Engineering of Japan, 24 (1991b) 581–586.

Iritani E., Itano Y., Murase T., Ultrafiltration of proteinaceous solutions by use of dynamic membranes formed by body-feed method, Membrane, 17 (1992) 203–206.

Iritani E., Tachi S., Murase T., Influence of protein adsorption on flow resistance of microfiltration membrane, Colloids and Surfaces A: Physicochemical and Engineering Aspects, 89 (1994) 15–22.

Iritani E., Mukai Y., Tanaka Y., Murase T., Flux decline behavior in dead-end microfiltration of protein solutions, Journal of Membrane Science, 103 (1995) 181–191.

Iritani E., Mukai Y., Hagihara E., Measurements and evaluation of concentration distributions in filter cake formed in dead-end ultrafiltration of protein solutions, Chemical Engineer-

ing Science, 57 (2002) 53–62.
Iritani E., Mukai Y., Furuta M., Kawakami T., Katagiri N., Blocking resistance of membrane during cake filtration of dilute suspensions, AIChE Journal, 51 (2005) 2609–2614.
Iritani E., Katagiri N., Sugiyama Y., Yagishita K., Analysis of flux decline behaviors in filtration of very dilute suspensions, AIChE Journal, 53 (2007a) 2275–2283.
Iritani E., Katagiri N., Sengoku T., Yoo K.M., Kawasaki K., Matsuda A., Flux decline behaviors in dead-end microfiltration of activated sludge and its supernatant, Journal of Membrane Science, 300 (2007b) 36–44.
Iritani E., Modeling and evaluation of pore clogging of membrane in membrane filtration, Kagaku Kogaku Ronbunshu, 35 (2009) 1–11.
Iritani E., Katagiri N., Tadama T., Sumi H., Analysis of clogging behaviors of diatomaceous ceramic membranes during membrane filtration based upon specific deposit, AIChE Journal, 56 (2010) 1748–1758.
Iritani E., Katagiri N., Sugiyama Y., Clogging properties of membrane pores in constant-rate and constant-pressure microfiltration of dilute colloids, Kagaku Kogaku Ronbunshu, 37 (2011) 323–326.
Iritani E., A review on modeling of pore-blocking behaviors of membranes during pressurized membrane filtration, Drying Technology, 31 (2013) 146–162.
Iritani E., Katagiri N., Tsukamoto M., Hwang K.J., Determination of cake properties in ultrafiltration of nano-colloids based on single step-up pressure filtration test, AIChE Journal, 60 (2014a) 289–299.
Iritani E., Katagiri N., Nakajima R., Hwang K.J., Cheng T.W., Cake properties of nanocolloid evaluated by variable pressure filtration associated with reduction in cake surface area, AIChE Journal, 60 (2014b) 3869–3877.
Iritani E., Katagiri N., Ishikawa Y., Cao D.Q., Cake formation and particle rejection in microfiltration of binary mixtures of particles with two different sizes, Separation and Purification Technology, 123 (2014c) 214–220.
Iritani E., Katagiri N, Takenaka T., Yamashita Y., Membrane pore blocking during cake formation in constant pressure and constant flux dead-end microfiltration of very dilute colloids, Chemical Engineering Science, 122 (2015) 465–473.
Ives K.J., Pienvichitr V., Kinetics of the filtration of dilute suspension, Chemical Engineering Science, 20 (1965) 965–973.
Jin Y., Ju Y., Lee H., Hong S., Fouling potential evaluation by cake fouling index: Theoretical development, measurements, and its implications for fouling mechanisms, Journal of Membrane Science, 490 (2015) 57–64.
Jonsson G., Prádanos P., Hernández A., Fouling phenomena in microporous membranes: Flux decline kinetics and structural modification, Journal of Membrane Science, 112 (1996) 171–183.
Juang R.S., Lin S.H., Peng L.C., Flux decline analysis in micellar-enhanced ultrafiltration of synthetic waste solutions for metal removal, Chemical Engineering Journal, 161 (2010) 19–26.
Katsoufidou K., Yiantsios S.G., Karabelas A.J., A study of ultrafiltration membrane fouling by humic acids and flux recovery by backwashing: Experiments and modeling, Journal of Membrane Science, 266 (2005) 40–50.
Keskinler B., Yildiz E., Erhan E., Dogru M., Bayhan Y.K., Akay G., Crossflow microfiltration of low concentration-nonliving yeast suspensions, Journal of Membrane Science, 233 (2004) 59–69.
Khirani S., Ben Aim R., Manero M.H., Improving the measurement of the modified fouling index using nanofiltration membranes (NF-MFI), Desalination, 161 (2006) 1–7.
Kim K.J., Chen V., Fane A.G., Ultrafiltration of colloidal silver particles: Flux, rejection, and fouling, Journal of Colloid and Interface Science, 155 (1993) 347–359.
Kim J., Shi W., Yuan Y., Benjamin M.N., A serial filtration investigation of membrane fouling by natural organic matter, Journal of Membrane Science, 294 (2007) 115–126.
Kimura S., Sourirajan S., Analysis of data in reverse osmosis with porous cellulose acetate membranes used, AIChE Journal, 13 (1967) 497–503.
Koo C.H., Mohammad A.W., Suja F., Meor Talib M.Z., Review of the effect of selected physicochemical factors on membrane fouling propensity based on fouling indices, Desalination, 287 (2012) 167–177.
Kozicki W., Chou C.H., Tiu C., Non-Newtonian flow in ducts of arbitrary cross-sectional shape, Chemical Engineering Science, 21 (1966) 665–679.
Kozicki W., Tiu C., Rao A.R.K., Filtration of non-Newtonian fluids, The Canadian Journal of Chemical Engineering, 46 (1968) 313–321.
Kozicki W., Rao A.R.K., Tiu C., Filtration of polymer solutions, Chemical Engineering Science, 27 (1972) 615–626.
Lee D.J., Filter medium clogging during cake filtration, AIChE Journal, 43 (1997) 273–276.
Lee S., Park P.K., Kim J.H., Yeon K.M., Lee C.H., Analysis of filtration characteristics in submerged microfiltration for drinking water treatment, Water Research, 42 (2008) 3109–3121.
Leu W.A., Tiller F.M., Experimental study of mechanism of constant pressure cake filtration: Clogging of filter media, Separation Science and Technology, 18 (1983) 1351–1369.
Li W.W., Sheng G.P., Wang Y.K., Lie X.W., Xu J., Yu H.Q., Filtration behaviors and biocake formation mechanism of mesh filters used in membrane bioreactors, Separation and Purification Technology, 81 (2011) 472–479.
Li F., Tian Q., Yang B., Wu L., Deng C., Effect of polyvinyl alcohol to model Extracellular Polymeric Substances (EPS) on membrane filtration performance, Desalination, 286 (2012) 34–40.
Lim A.L., Bai R., Membrane fouling and cleaning in microfiltration of activated sludge wastewater, Journal of Membrane Science, 216 (2003) 279–290.
Lim Y.P., Mohammad A.W., Influence of pH and ionic strength during food protein ultrafiltration: Elucidation of permeate flux behaviors, fouling resistance, and mechanism, Separation Science and Technology, 47 (2012) 446–454.
Liu Q.F., Kim S.H., Evaluation of membrane fouling models based on bench-scale experiments: A comparison between constant flowrate blocking laws and artificial neural net-

work (ANNs) model, Journal of Membrane Science, 310 (2008) 393–401.

Ma N., Zhang Y., Quan X., Fan X., Zhao H., Performing a microfiltration integrated with photocatalysis using an Ag-TiO_2/HAP/Al_2O_3 composite membrane for water treatment: Evaluating effectiveness for humic acid removal and anti-fouling properties, Water Research, 44 (2010) 6104–6114.

Madaeni S.S., Fane A.G., Microfiltration of very dilute colloidal mixtures, Journal of Membrane Science, 113 (1996) 301–312.

Mahdi F.M., Holdich R.G., Laboratory cake filtration testing using constant rate, Chemical Engineering Research and Design, 91 (2013) 1145–1154.

Maroudas A., Eisenklam P., Clarification of suspensions: A study of particle deposition in granular media, Part II—A theory of clarification, Chemical Engineering Science, 20 (1965) 875–888.

Masoudnia K., Raisi A., Aroujalinan A., Fathizadeh M., Treatment of oily wastewaters using the microfiltration process: Effect of operating parameters and membrane fouling study, Separation Science and Technology, 48 (2013) 1544–1555.

Matsumoto K., Hirata S., Ohya H., Microfiltration model considering incomplete pore blocking and incomplete capture of particles by cake, Kagaku Kogaku Ronbunshu, 18 (1992) 455–462.

Matsumoto K., Furuichi M., Nakamura K., Nittami T., Evaluation of water quality by the modified SDI in the membrane filtration process, Membrane, 34 (2009) 94–103.

Mohammadi T., Kohpeyma A., Sadrzadeh M., Mathematical modeling of flux decline in ultrafiltration, Desalination, 184 (2005) 367–375.

Mohd Amin I.N.H., Mohammad A.W., Marcom M., Peng L.C., Hilal N., Analysis of deposition mechanism during ultrafiltration of glycerin-rich solutions, Desalination, 261 (2010) 313–320.

Mondal S., De S., Generalized criteria for identification of fouling mechanism under steady state membrane filtration, Journal of Membrane Science, 344 (2009) 6–13.

Murase T., Iritani E., Cho J.H., Nakanomori S., Shirato M., Determination of filtration characteristics due to sudden reduction in filtration area of filter cake surface, Journal of Chemical Engineering of Japan, 20 (1987) 246–251.

Murase T., Iritani E., Cho J.H., Shirato M., Determination of filtration characteristics of power-law non-Newtonian fluids-solids mixtures under constant-pressure conditions, Journal of Chemical Engineering of Japan, 22 (1989) 65–71.

Murase T., Ohn, T., New decline pattern of filtrate flux in cross-flow microfiltration of dilute suspension, AIChE Journal, 42 (1996) 1938–1944.

Nagel R., Seawater desalination with polyamide hollow fibre modules at DROP, Desalination, 63 (1987) 225–246.

Nakakura H., Yamashita A., Sambuichi M., Osasa K., Electrical conductivity measurement of filter cake in dead-end ultrafiltration of protein solution, Journal of Chemical Engineering of Japan, 30 (1997) 1020–1025.

Nakamura K., Orie T., Matsumoto K., Response of zeta potential to cake formation and pore blocking during the microfiltration of latex particles, Journal of Membrane Science, 401–402 (2012) 274–281.

Nandi B.K., Moparthi A., Uppaluri R., Purkait M.K., Treatment of oily wastewater using low cost ceramic membrane: Comparative assessment of pore blocking and artificial neural network models, Chemical Engineering Research and Design, 88 (2010) 881–892.

Notebaert F.F., Wilms D.A., van Haute A.A., A new deduction with a larger application of the specific resistance to filtration of sludges, Water Research, 9 (1975) 667–673.

Okamura S., Shirato M., Liquid pressure distribution within cakes in the constant pressure filtration, Kagaku Kogaku, 19 (1955) 104–110.

Ozdemir B., Saatci A., Yenigun O., Evaluation of cake filtration biological reactors (CFBR) vs. membrane biological reactor (MBR) in a pilot scale plant, Desalination, 288 (2012) 135–144.

Palacio L., Ho C.C., Zydney A.L., Application of a pore-blockage—cake-formation model to protein fouling during microfiltration, Biotechnology and Bioengineering, 79 (2002) 260–270.

Palacio L., Ho C.C., Prádanos P., Hernández A., Zydney A.L., Fouling with protein mixtures in microfiltration: BSA-lysozyme and BSA-pepsin, Journal of Membrane Science, 222 (2003) 41–51.

Palencia M., Rivas B.L., Valle H., Size separation of silver nanoparticles by dead-end ultrafiltration: Description of fouling mechanism by pore blocking model, Journal of Membrane Science, 455 (2014) 7–14.

Park C., Kim H., Hong S., Choi S.I., Variation and prediction of membrane fouling index under various feed water characteristics, Journal of Membrane Science, 284 (2006) 248–254.

Pan Y., Wang T., Sun H., Wang W., Preparation and application of titanium dioxide dynamic membranes in microfiltration of oil-in-water emulsions, Separation and Purification Technology, 89 (2012) 78–83.

Persson A., Jönsson A.S., Zacchi G., Transmission of BSA during cross-flow microfiltration: Influence of pH and salt concentration, Journal of Membrane Science, 223 (2003) 11–21.

Polyakov Y.S., Depth filtration approach to the theory of standard blocking: Prediction of membrane permeation rate and selectivity, Journal of Membrane Science, 322 (2008) 81–90.

Polyakov Y.S., Zydney A.L., Ultrafiltration membrane performance: Effects of pore blockage/constriction, Journal of Membrane Science, 434 (2013) 106–120.

Prádanos P., Hernández A., Calvo J.I., Tejerina F., Mechanisms of protein fouling in cross-flow UF through an asymmetric inorganic membrane, Journal of Membrane Science, 114 (1996) 115–126.

Purkait M.K., DasGupta S., De S., Resistance in series model for micellar enhanced ultrafiltration of eosin dye, Journal of Colloid and Interface Science, 270 (2004) 496–506.

Purkait M.K., Bhattacharya P.K., De S., Membrane filtration of leather plant effluent: Flux decline mechanism, Journal of

membrane Science, 258 (2005) 85–96.
Rai P., Majumdar G.C., Sharma G., DasGupta S., De S., Effect of various cutoff membranes on permeate flux and quality during filtration of Mosambi (*Citrus Sinensis* (L.) Osbeck) juice, Transactions of The Institution of Chemical Engineers, Part C, Food and Bioproducts Processing, 84 (2006) 213–219.
Raspati G.S., Meyn T., Leiknes T., Analysis of membrane and cake layer resistances in coagulation: Constant flux dead-end microfiltration of NOM, Separation Science and Technology, 48 (2013) 2252–2262.
Reihanian H., Robertson C.R., Michaels A.S., Mechanism of polarization and fouling of ultrafiltration membranes by proteins, Journal of Membrane Science, 16 (1983) 237–258.
Rezaei H., Ashtiani F.Z., Fouladitajar A., Effects of operating parameters on fouling mechanism and membrane flux in cross-flow microfiltration of whey, Desalination, 274 (2011) 262–271.
Rodgers V.G.J., Oppenheim S.F., Datta R., Correlation of permeability and solute uptake in membranes of arbitrary pore morphology, AIChE Journal, 41 (1995) 1826–1829.
Ruohomäki K., Nyström M., Fouling of ceramic capillary filters in vacuum filtration of humic acid, Filtration + Separation, 37(1) (2000) 51–57.
Rushton A., The flow and filtration of non-Newtonian fluids (Part A), Filtration & Separation, 10 (1986) 41–43.
Ruth B.F., Studies in filtration, III. Derivation of general filtration equations, Industrial & Engineering Chemistry, 27 (1935) 708–723.
Ruth B.F., Correlating filtration theory with industrial practice, Industrial & Engineering Chemistry, 38 (1946) 564–571.
Salinas-Rodriguez S.G., Amy G.L., Schippers J.C., Kennedy M.D., The Modified Fouling Index Ultrafiltration constant flux for assessing particulate/colloidal fouling of RO systems, Desalination, 365 (2015) 79–91.
Sarkar B., De S., A combined complete pore blocking and cake filtration model for steady-state electric field-assisted ultrafiltration, AIChE Journal, 58 (2012) 1435–1446.
Sarkar B., A combined complete pore blocking and cake filtration model during ultrafiltration of polysaccharide in a batch cell, Journal of Food Engineering, 116 (2013) 333–343.
Schippers J.C., Hanemaayer J.H., Smolders C.A., Kostense A., Predicting flux decline of reverse osmosis membranes, Desalination, 38 (1981) 339–348.
Shirato M., Aragaki T., Mori R., Sawamoto K., Predictions of constant pressure and constant rate filtrations based upon an approximate correction for side wall friction in compression permeability cell data, Journal of Chemical Engineering of Japan, 1 (1968) 86–90.
Shirato M., Sambuichi M., Kato H., Aragaki T., Internal flow mechanism in filter cakes, AIChE Journal, 15 (1969) 405–409.
Shirato M., Aragaki T., Iritani E., Wakimoto M., Fujiyoshi S., Nanda S., Constant pressure filtration of power-law non-Newtonian Fluids, Journal of Chemical Engineering of Japan, 10 (1977) 54–60.
Shirato M., Aragaki T., Iritani E., Blocking filtration laws for filtration of power-law non-Newtonian fluids, Journal of Chemical Engineering of Japan, 12 (1979) 162–164.
Shirato M., Aragaki T., Iritani E., Analysis of constant pressure filtration of power-law non-Newtonian fluids, Journal of Chemical Engineering of Japan, 13 (1980) 61–66.
Sperry D.R., Note and correspondence: A study of the fundamental laws of filtration using plant-scale equipment, Industrial & Engineering Chemistry, 13 (1921) 1163–1164.
Srisukphun T., Chiemchaisri C., Yamamoto K., Modeling of RO flux decline in textile wastewater reclamation plants using variable fouling index, Separation Science and Technology, 44 (2009) 1704–1721.
Suarez J.A., Veza J.M., Dead-end microfiltration as advanced treatment for wastewater, Desalination, 127 (2000) 47–58.
Sun S., Yue Y., Huang X., Meng D., Protein adsorption on blood contact membranes, Journal of Membrane Science, 222 (2003) 3–18.
Sun X., Kanani D.M., Ghosh R., Characterization and theoretical analysis of protein fouling of cellulose acetate membrane during constant flux dead-end microfiltration, Journal of Membrane Science, 320 (2008) 372–380.
Takahashi K., Ohmori N., Ishi K., Yokota T., Cake formation and spatial partitioning in batch microfiltration of yeast, Journal of Chemical Engineering of Japan, 24 (1991) 372–377.
Taniguchi M., Kilduff J.E., Belfort J., Modes of natural organic matter fouling during ultrafiltration, Environmental Science & Technology, 37 (2003) 1676–1683.
Tettamanti B., Modeling and scaling of filtration in industry, International Chemical Engineering, 22 (1982) 561–571.
Thekkedath A., Naceur W.M., Kecili K., Sbai M., Elane A., Auret L., Suty H., Machinal C., Pontié M., Macroscopic and microscopic characterization of a cellulosic ultrafiltration (UF) membrane fouled by a humic acid cake deposit: First step for intensification of reverse osmosis (RO) pre-treatments, Comptes Rendus Chimie, 10 (2007) 803–812.
Tien C., Payatakes A.C., Advances in deep bed filtration, AIChE Jornal, 25 (1979) 737–759.
Tien C., Ramarao B.V., Revisiting the laws of filtration: An assessment of their use in identifying particle retention mechanisms in filtration, Journal of Membrane Science, 383 (2011) 17–25.
Tien C., Ramarao B.V., Yasarla R., A blocking model of membrane filtration, Chemical Engineering Science, 111 (2014) 421–431.
Tiller F.M., The role of porosity in filtration, I. Numerical methods for constant rate and constant pressure filtration based on Kozeny's law, Chemical Engineering Progress, 49 (1953) 467–479.
Tiller F.M., The role of porosity in filtration, Part 2, Analytical equations for constant rate filtration, Chemical Engineering Progress, 51 (1955) 282–290.
Tiller F.M., Cooper H.R., The role of porosity in filtration: IV. Constant pressure filtration, AIChE Journal, 6 (1960) 595–601.
Tiller F.M., Shirato M., The role of porosity in filtration: VI. New definition of filtration resistance, AIChE Journal, 10

(1964) 61–67.
Tiller F.M., Weber W., Davies O., Clogging phenomena in the filtration of liquefied coal, Chemical Engineering Progress, 77(Dec.) (1981) 61–68.
Todisco S., Peña L., Drioli, E., Tallarico P., Analysis of the fouling mechanism in microfiltration of orange juice, Journal of Food Processing and Preservation, 20 (1996) 453–466.
Tracey E.M., Davis R.H., Protein fouling of track-etched polycarbonate microfiltration membranes, Journal of Colloid and Interface Science, 167 (1994) 104–116.
van Reis R., Zydney A., Bioprocess membrane technology, Journal of Membrane Science, 297 (2007) 16–50.
Vera M.C.V., Blanco S.Á., García J.L., Rodríguez E.B., Analysis of membrane pore blocking models adapted to crossflow ultrafiltration in the ultrafiltration of PEG, Chemical Engineering Journal, 149 (2009) 232–241.
Vilker V.L., Colton C.K., Smith K.A., Concentration polarization in protein ultrafiltration, AIChE Journal, 27 (1981) 632–645.
Wang F., Tarabara V.V., Pore blocking mechanisms during early stages of membrane fouling by colloids, Journal of Colloid and Interface Science, 328 (2008) 464–469.
Wei C.H., Laborie S., Ben Aim R., Amy G., Full utilization of silt density index (SDI) measurements for seawater pretreatment, Journal of Membrane Science, 405–406 (2012) 212–218.
White D.A., The interpretation of the SDI for water solids content using the filtration equation, Transactions of the Institution of Chemical Engineers, Part B, Process Safety and Environmental Protection, 74 (1996) 137–140.
Wu J., He C., Zhang Y., Modeling membrane fouling in a submerged membrane bioreactor by considering the role of solid, colloidal and soluble components, Journal of Membrane Science, 397–398 (2012) 102–111.
Ye Y., Clech P.L., Chen V., Fane A.G., Jefferson B., Fouling mechanisms of alginate solutions as model extracellular polymeric substances, Desalination, 175 (2005) 7–20.
Yiantsios S.G., Karabelas A.J., An assessment of the Silt Density Index based on RO membrane colloidal fouling experiments with iron oxide particles, Desalination, 151 (2003) 229–238.
Yukseler H., Tosun I., Yetis U., A new approach in assessing slurry filterability, Journal of Membrane Science, 303 (2007) 72–79.
Yuan W., Kocic A., Zydney A.L., Analysis of humic acid fouling during microfiltration using a pore blockage – cake filtration model, Journal of Membrane Science, 198 (2002) 51–62.
Zeman L.J., Adsorption effects in rejection of macromolecules by ultrafiltration membranes, Journal of Membrane Science, 15 (1983) 213–230.
Zhong Z., Li W., Zing W., Xu N., Crossflow filtration of nanosized catalysis suspension using ceramic membranes. Separation and Purification Technology, 76 (2011) 223–230.
Zhou J., Wandera D., Husson S.M., Mechanisms and control of fouling during ultrafiltration of high strength wastewater without pretreatment, Journal of Membrane Science, 488 (2015) 103–110.

Author's short biography

Eiji Iritani

Eiji Iritani is currently Professor of Department of Chemical Engineering at Nagoya University. He received his Docter degree of Engineering from Nagoya University in 1981. His research interests are in the area of cake filtration, membrane filtration, deliquoring due to expression, sedimentation, centrifugation, and water treatments based on solid-liquid separation technology.

Nobuyuki Katagiri

Nobuyuki Katagiri is currently Assistant Professor of Department of Chemical Engineering at Nagoya University. He received his Doctor degree of Agriculture from Gifu University in 1998. His research interests are in the area of filtration and expression of biologically-derived materials, and waste water treatments.